Published in final edited form as:
Dev Biol. 2009 May 15; 329(2): 212–226. doi:10.1016/j.ydbio.2009.02.031.

A genetic screen for vascular mutants in zebrafish reveals dynamic roles for Vegf/Plcg1 signaling during artery development

L. D. Covassin[1], **A. F. Siekmann**[1], **M. C. Kacergis**[1], **E. Laver**[1], **J. C. Moore**[1], **J. A. Villefranc**[1], **B. M. Weinstein**[2], and **N. D. Lawson**[1,*]

[1] Program in Gene Function and Expression, University of Massachusetts Medical School, Worcester, MA

[2] Laboratory of Molecular Genetics, NICHD, NIH, Bethesda, MD

Abstract

In this work we describe a forward genetic approach to identify mutations that affect blood vessel development in the zebrafish. By applying a haploid screening strategy in a transgenic background that allows direct visualization of blood vessels, it was possible to identify several classes of mutant vascular phenotypes. Subsequent characterization of mutant lines revealed that defects in Vascular endothelial growth factor (Vegf) signaling specifically affected artery development. Comparison of phenotypes associated with different mutations within a functional zebrafish Vegf receptor-2 ortholog (referred to as *kdr-like, kdrl*) revealed surprisingly varied effects on vascular development. In parallel, we identified an allelic series of mutations in *phospholipase c gamma 1 (plcg1)*. Together with *in vivo* structure-function analysis, our results suggest a requirement for Plcg1 catalytic activity downstream of receptor tyrosine kinases. We further find that embryos lacking both maternal and zygotic *plcg1* display more severe defects in artery differentiation but are otherwise similar to zygotic mutants. Finally, we demonstrate through mosaic analysis that *plcg1* functions autonomously in endothelial cells. Together our genetic analyses suggest that Vegf/Plcg1 signaling acts at multiple time points and in different signaling contexts to mediate distinct aspects of artery development.

Introduction

The circulatory system provides oxygenation and waste removal for developing organs and tissues, while serving as a conduit for hormones and components of the immune system (Cleaver and Krieg, 1999). In addition, the endothelial cells lining nascent blood vessels also serve as a source for important inductive and guidance signals during organogenesis (Alt et al., 2006; Lammert et al., 2001). Accordingly, blood vessel function is essential for vertebrate embryonic development (Cleaver and Krieg, 1999). As organisms transition from embryonic to adult stages, new blood vessel formation (neovascularization) becomes more limited and in most cases this process is associated with pathological conditions in the adult. As with normal tissue and organs during embryonic development, ischemic tissue or nascent tumors require increased vascularization and are known to produce and secrete numerous angiogenic molecules that promote blood vessel growth (Semenza, 2003). In most cases, the signals that

*corresponding author: Nathan D. Lawson, Ph.D., Associate Professor, Program in Gene Function and Expression, University of Massachusetts Medical School, Lazare Research Building, Room 617, 364 Plantation Street, Worcester, MA 01605, Phone: (508) 856-1177, nathan.lawson@umassmed.edu.

promote neovascularization in these pathological settings in adults are the same that are used by the embryo (Cleaver and Krieg, 1999). Furthermore, the signaling molecules and cellular mechanisms by which blood vessels form have been evolutionarily conserved (Weinstein and Lawson, 2002). Accordingly, it is has been possible to gain significant insights on pathological blood vessel formation through the study of embryonic vascular development in vertebrate model systems.

Among the important signaling molecules that are responsible for neovascularization in both embryonic and adult settings are several receptor tyrosine kinase families. These include receptors for vascular endothelial growth factors (Vegf), angiopoietins and the membrane-bound ephrin ligands (Yancopoulos et al., 2000). Vegf-A initiates and induces endothelial cell differentiation at the earliest stages of blood vessel development (Ferrara et al., 2003). Vegf-A acts by binding Vegfr-2, an endothelial cell specific receptor tyrosine kinase (Quinn et al., 1993). Mice lacking either Vegf-A or Vegfr-2 display severely reduced numbers of endothelial cells and fail to form blood vessels (Carmeliet et al., 1996; Shalaby et al., 1995). Loss of specific Vegf-A isoforms or endothelial autonomous ablation of Vegf signaling has revealed later roles for this signaling pathway in arterial endothelial cell differentiation and promoting endothelial cell survival, respectively (Carmeliet et al., 1999; Lawson et al., 2002; Lee et al., 2007; Stalmans et al., 2002). Furthermore, Vegf-A is also required for angiogenic sprouting and plays an important role in modulating vascular permeability in both adult and embryonic stages (Bates and Harper, 2002; Ferrara et al., 2003). In parallel to the Vegf signaling pathway, the angiopoietins and their receptor, Tie2, mediate subsequent sprouting and maturation of the vascular network at later stages of embryonic development. Angiopoietin/Tie2 signaling plays an important role in crosstalk between endothelial cells lining the blood vessels and associated vascular smooth muscle cells during angiogenic sprouting (Davis et al., 1996; Maisonpierre et al., 1997; Suri et al., 1996; Suri et al., 1998). Similarly, the Eph receptor tyrosine kinases and their ligands, referred to as ephrins, mediate cell-cell signaling between distinct cell types in the developing vascular system (Yancopoulos et al., 1998). Eph-ephrin signaling plays an important role in mediating the interface and separation between arteries and veins (Gerety et al., 1999; Wang et al., 1998), as well as endothelial cell interaction with surrounding mesenchymal cells (Adams et al., 1999; Yancopoulos et al., 1998).

For the most part, the functional analysis of these and other signaling pathways during vascular development has proceeded largely through reverse genetic approaches using the mouse as a model system. More recently, the zebrafish has emerged as an ideal model system for studying embryonic vascular development (Roman and Weinstein, 2000). The transparency and external fertilization of the zebrafish embryo, coupled with the use of endothelial cell-specific fluorescent protein transgenes have allowed an unprecedented view of blood vessel formation in a live organism (Beis and Stainier, 2006; Lawson and Weinstein, 2002; Roman et al., 2002; Siekmann et al., 2008). These particular aspects of the zebrafish embryo have made it a tractable vertebrate model for forward genetic screening. Early screens relying on the straightforward visualization of blood circulation in the zebrafish embryo led to the identification of mutations that affected cardiovascular morphogenesis or function (Chen et al., 1996; Stainier et al., 1996). More recently, the use of transgene-assisted screens (Jin et al., 2007) has allowed more subtle characterization of defective vascular phenotypes in mutant zebrafish embryos. The ability to easily generate thousands of progeny embryos coupled with the increasing quality of genomics tools has facilitated genetic mapping and identification of genes responsible for many of these phenotypes (Patton and Zon, 2001).

In this study, we describe a haploid transgenic screen in zebrafish embryos to identify mutants that perturb normal vascular development. This screening approach allowed robust and specific detection of several different classes of mutant vascular phenotypes and the majority of these were subsequently observed in diploid embryos. Subsequent characterization and cloning of

the genes responsible for these mutant phenotypes revealed that the zebrafish Vegf receptor, *kdr-like* (*kdrl*), and *phospholipase c gamma 1* (*plcg1*) were essential for artery development. Interestingly, detailed phenotypic analysis of different *kdrl* alleles suggested diverse roles for this receptor during development of blood vessels. Parallel analysis of *plcg1* alleles, along with *in vivo* structure/function experiments, indicated a crucial role for Plcg1 catalytic function downstream of receptor tyrosine kinases during artery development. Furthermore, analysis of maternal-zygotic *plcg1* mutant embryos suggested an early role for Vegf/Plcg1 signaling during arterial specification, while mosaic analysis revealed an endothelial autonomous role for *plcg1* during vascular morpohgenesis. Taken together our results demonstrate the utility of a transgenic haploid screening approach to identify mutants affecting vascular development in the zebrafish and underscore the diverse roles of Vegf/Plcg1 signaling during artery development.

Materials and methods

Fish handling and care

All zebrafish were maintained according to standard protocols (Westerfield, 1993) and in accordance with University of Massachusetts Medical School IACUC guidelines.

Transgenic and mutant lines

Nomenclature for the zebrafish Vegf receptor orthologs was assigned based on recently described guidelines (Bussmann et al., 2008). The *um19* allele is a 4 base pair deletion in exon 2 of *kdrl* that was generated by targeted mutagenesis using zinc finger nucleases and is described elsewhere (Meng et al., 2008). The *Tg(fli1a:egfp)*^{y1} line has been described elsewhere (Lawson and Weinstein, 2002). To generate zebrafish embryos with red fluorescent blood vessels, we constructed a plasmid containing a chimeric endothelial enhancer-promoter fragment driving dsRed-Express via Gateway cloning into a Tol2 plasmid backbone (Villefranc et al., 2007). The resulting plasmid (pTol*fli1ep:dsredex*) was co-injected into 1-cell stage wild type zebrafish embryos along with mRNA encoding the Tol2 Transposase (Kawakami et al., 2004). Embryos with the highest and least mosaic expression were grown to adulthood and founders were identified by out-crossing. The *Tg(fli1ep:dsredex)*^{um13} line was derived from a single founder.

Mutagenesis and screening

ENU mutagenesis was performed based on previously described protocols (Solnica-Krezel et al., 1994). Briefly, we treated homozygous *Tg(fli1a:egfp)*^{y1} adult males with 3 mM N-ethyl-N-nitrosourea (ENU) for 1 hour once a week for a total of 4 weeks. Following a two-week recovery, fish were bred to wild type females to purge mutagenized gametes that usually harbor gross chromosomal aberrations (Imai et al., 2000). ENU-treated males were then crossed to homozygous *Tg(fli1a:egfp)*^{y1} females to generate an F1 generation. Beginning at 6 months of age, F1 *Tg(fli1a:egfp)*^{y1} females were used to generate haploid embryos by performing *in vitro* fertilization (Westerfield, 1993) using UV irradiated sperm. Each individual F1 *Tg (fli1a:egfp)*^{y1} female that successfully gave viable haploids was maintained in an individual tank. Subsequently, *Tg(fli1a:egfp)*^{y1} embryos were screened at 30 hours post fertilization and again at 50 hpf for defects in segmental artery formation, as well as overall morphology using a stereo dissection microscope equipped with epifluorescence. F1 *Tg(fli1a:egfp)*^{y1} females that gave clutches of embryos in which fifty percent displayed a mutant vascular phenotype were subsequently out-crossed to TL males to generate a map cross. Females that gave mutant phenotypes that exhibited general morphological defects or necrosis were not maintained. Genetic linkage mapping and candidate cloning of genes was carried out as described elsewhere (Lawson et al., 2003; Roman et al., 2002).

Phenotypic analysis and microscopy

All diploid mutant embryos were analyzed at 30 hpf using a dissection microscope equipped with epifluorescence (Leica MZFLIII, 1x PlanApo) to determine presence of segmental arteries. Embryos were also observed with transmitted light at 55 hpf to observe circulatory patterns and overall morphology. Vascular morphology defects were documented in more detail using a Leica DMIRE2 microscope equipped with a TCS SP2 confocal laser scanning system (Objective: HC PL APO 20x/0.70 CS, dry). In most cases, vertical projections of confocal stacks were generated using Leica Confocal Software (LCS). Alternatively, vertical projections were generated using the Imaris software package (Bitplane). Sprout length was measured in 3-dimensional stacks using Imaris. For this purpose, 6 pairs of segmental artery sprouts were counted in at least 3 embryos from 3 different clutches. Length was measured as distance of a perpindicular line from the dorsal wall of the dorsal aorta to the distal end of the segmental artery. Overall morphology was documented by capturing digital images using transmitted light on a MZFLIII dissection microscope equipped with a Zeiss Axiocam mRC digital camera using Axiovision software (Zeiss). More detailed morphological imaging was performed by differential interference contrast (DIC) microscopy using a Zeiss Axioskop2plus compound microscope (Achroplan 20x/0.5 water; Achroplan 40x/0.8 water) equipped with a Zeiss Axiocam hRC digital camera. All images were exported from Axiovision, LCS, or Imaris as TIF files and imported into Photoshop CS2 (Adobe) to generate figures.

Riboprobes

Antisense riboprobes against *ephrinb2a*, *dll4*, and *notch3*, were generated as described previously (Lawson et al., 2001; Siekmann and Lawson, 2007). Whole mount *in situ* hybridization was performed as described elsewhere (Hauptmann and Gerster, 1994). DIC images of stained embryos were captured as described above.

Generation of germ cell plcg1 mutants

To generate adults bearing *plcg1* deficient germ cells, we utilized the germ-line replacement strategy described elsewhere (Ciruna et al., 2002). Briefly, embryos from an incross of non-transgenic *plcg1*^{y18} carriers were injected with mRNA encoding EGFP with the 3′UTR from the *nanos* transcript. In parallel, wild type embryos were injected with a morpholino targeting the *dead end* gene to ablate host germ cells. Donor cells from the margin of sphere stage embryos derived from putative *plcg1*^{y18} carriers were transplanted into the margin of host wild type embryos. Donor and host embryos were then allowed to develop until 24 to 48 hpf. Host embryos were grown to adulthood if the corresponding donor embryo was found to be mutant for *plcg1* by visual inspection and the host embryos displayed evidence of transplanted germ cells as indicated by green fluorescence. Putative maternal (M) or paternal (P) mutant founders were identified by crossing them to heterozygous *plcg1*^{y18} mutant carriers. In all cases, M*plcg1*^{y18} and P*plcg1*^{y18} carriers displayed fully penetrant *plcg1* mutant phenotypes indicating that all germ cells were mutant.

Plcg1 rescue experiments

Previously described mutations in the SH2 (Ji et al., 1999) and SH3 (Ye et al., 2002) domains of Plcg1 were introduced into zebrafish *plcg1* coding sequence by overlapping PCR and all constructs were validated by sequencing. Mutant constructs were generated in the pCS-mtplcg1 backbone (Lawson et al., 2003). All plasmids were linearized with Not I and mRNA synthesized using the mMessage mMachine kit (Ambion) to drive transcription from the SP6 promoter. We injected 400 pg of mRNA into 1-cell stage embryos derived from an incross of *plcg1*^{y18} heterozygous carriers. As controls, embryos were injected with mRNA encoding wild type Plcg1, or left uninjected. Embryos were scored at 30 hpf for segmental artery formation; embryos were classified as having no segmental arteries (SeA−), partial segmental arteries,

with no dorsal longitudinal anastomotic vessel (SeA+DLAV−), or wild type (SeA+DLAV+). At 55 hpf, embryos were scored for blood circulation and classified with normal circulation (circ+), evidence of shunting between the dorsal aorta and posterior cardinal vein (partial), or no circulation (circ−). Following phenotypic analysis, all embryos were subjected to PCR-screening for genotyping.

To generate expression constructs for activated forms of Akt or MAP2K1, we first generated Gateway entry clones. A constitutively membrane-localized form of Akt was PCR-amplified from a plasmid template (kindly provided by Fumihiko Urano, UMass Medical School) using the following primers: 5′-GGGGACAAGTTTGTACAAAAAAGCAGGCTCCGCGTTTAGCTT**ATG**GGGAG and 5′-GGGGACCACTTTGTACAAGAAAGCTGGGTAGGCTGTGCCACTGGCTGAGT, where Akt coding sequence are underlined and the endogenous start codon is in bold. An activated form of human MAP2K1 was amplified from plasmid template (kindly provided by Roger Davis, UMass Medical School) using primers 5′-GGGGACAAGTTTGTACAAAAAAGCAGGCTccAAA**ATG**CCCAAGAAGAAGC and 5′-GGGGACCACTTTGTACAAGAAAGCTGGGTTTAGACGCCAGCAGCATGGGT; hMAP2K1 sequence is underlined, endogenous start codon is in bold. In both cases, the forward primer contains an attB1 site, while the reverse primer contains an attB2 site. PCR products were subjected to BP cloning to generate pMEmAkt and pMEactMAP2K1 entry clones, which were sequence validated. Entry clones were then used in Gateway LR reactions to generate expression clones. For actMAP2K1, we constructed N-terminal monomeric Cherry fusion proteins by recombining pMEactMAP2K1 with either pCSCherDest (to give pCS-*mcher-actMAP2K1*)or pTolfli1epCherDest (to give pTol-*fli1ep:mcher-actMAP2K1*) (Villefranc et al., 2007). For mAkt, we utilized multisite Gateway cloning to generate a tandem, unfused mAkt-mCherry cassette using the viral 2A peptide sequence (Provost et al., 2007). For this purpose, we recombined pMEmAkt with pCSDest2 (Villefranc et al., 2007) and p3E-*2a-mcherry* (kindly provided by Chi-Bin Chien, University of Utah) to give pCS-*mAkt-2a-mcher*. To generate an endothelial cell specific construct, we recombined pMEmAkt with p5E*fli1ep*, which contains a chimeric fragment of a *fli1a* enhancer and promoter (Villefranc et al., 2007), pDest Tol2pA (Kwan et al., 2007), and p3E-*2a-mcherry* to give pTol-*fli1ep:mAkt-2a-mcherry*. We utilized pCS-*mCher-actMAP2K1* and pCS-*mAkt-2a-mcherry* for mRNA synthesis as described elsewhere (Villefranc et al., 2007) and mRNA was injected at 1- to 2-cell stage into wild type embryos. For pTol-*fli1ep:mAkt-2a-mcher* and pTol-*fli1ep:mcher-actMAP2K1*, we co-injected 25 pg of circular plasmid DNA with 25 pg Tol2 *transposase* mRNA into 1-cell stage embryos derived from an incross of *plcg1*^{y13} heterozygous carriers. Injected embryos were observed for segmental artery formation and circulation as described above.

Genotyping

The *plcg1*^{y13} mutation eliminates a *Pst*I site within the X-catalytic domain. PCR was performed using primers 5′-CTGCGTTCAGCTATCCCATC and 5′-CCTCTTGAGCTGGTGTGGCGA and the resulting product was digested with *Pst*I. The *plcg1*^{y16} mutation eliminates an *Eag*I in the N-terminal SH2 domain. For *y16* genotyping, primers 5′-GTATGGACCAGCATGTGACGGAG and 5′-CTACAAAGGTCTCGCTCTCCCGC were used for PCR and the resulting fragment was digested with EagI. For genotyping the *plcg1*^{y18} allele, we amplified a CA repeat within *plcg1* (primers: 5′-TGTAGGATCTGAGGTTTGAT and 5′ TGAGATCCTTGAGCCTGGGG) that was polymorphic in our background strain. Alternatively, we utilized a single nucleotide polymorphism (SNP) within a StyI site in *plcg1* in our crosses (5′-GCAACGAGTTCGAGATGAAGC and 5′-GTGTGGACGCATAGCCCTC). Genotyping of

the *kdrl* alleles was performed as described elsewhere (Covassin et al., 2006; Meng et al., 2008).

Mosaic analysis

For mosaic analysis of *plcg1* deficient cells in wild type vasculature, donor *Tg(fli1a:egfp)^{y1}* embryos were prepared by injecting with the lineage tracer Cascade Blue (Molecular Probes/Invitrogen) and 7.5 ng of a plcg1 morpohlino targeting the exon 1 splice donor site (Lawson et al., 2003) at 1- to 2-cell stage. At sphere stage, cells were removed from donor embryos and transferred to wild type *Tg(fli1ep:dsredex)^{um13}* hosts using a glass capillary. For analysis of wild type cells in *plcg1*-deficient vasculature, donor *Tg(fli1a:egfp)^{y1}* embryos were injected with the lineage tracer Cascade Blue. Subsequently, donor cells were placed into *Tg(fli1ep:dsredex)^{um13}* embryos that had been injected at the 1-cell stage with the *plcg1* morpohlino. As a control, cells for Cascade Blue-injected wild type *Tg(fli1a:egfp)^{y1}* embryos were transplanted into uninjected wild type *Tg(fli1ep:dsredex)^{um13}* host embryos. In all cases, embryos were grown to 26 to 28 hpf at which time position of GFP+ donor cells was determined through visualization by confocal microscropy as described above. Emission from GFP, dsRedEx, and Cascade Blue was acquired by sequential scanning using a 488 nm, 561 nm and 405 nm laser line, respectively. Subsequently, confocal stacks were used to generate vertical projection and overlays using the included Leica software, Imaris, or Photoshop CS2.

Results

A haploid transgenic screen to identify mutants that affect embryonic vascular development

Previous forward screening strategies to identify vascular mutants in zebrafish have relied on observation of circulatory defects in F3 embryos as a primary screen (Chen et al., 1996; Jin et al., 2007; Stainier et al., 1996). However, the two-generation breeding scheme used in F3 screens is labor- and cost-intensive and can take several years to screen sufficient numbers of genomes. In an effort to more easily screen for vascular mutants in zebrafish, we took advantage of the ability to generate haploid embryos to allow screening of progeny from F1 females. Additionally, we utilized *Tg(fli1a:egfp)^{y1}* zebrafish (Lawson and Weinstein, 2002) to allow direct visualization of putative vascular phenotypes in developing haploid embryos derived from F1 females.

To induce mutations in the male zebrafish germline, we treated homozygous *Tg(fli1a:egfp)^{y1}* males with N-ethyl-N-nitrosourea (ENU). Subsequently, we used ENU-treated males to generate F1 families (Figure 1A). To identify mutations that would lead to blood vessel defects, we generated haploid embryos from individual *Tg(fli1a:egfp)^{y1}* F1 females and screened for segmental artery formation at 1 or 2 days post fertilization. In general, we found that the overall morphology of haploid *Tg(fli1:egfp)^{y1}* zebrafish embryos was relatively normal, although body length was shortened and somite formation, as well as head development was often mildly perturbed (Fig. 1B and data not shown). Despite these mild abnormalities, trunk blood vessel morphology and segmental artery formation was robust in wild type *Tg(fli1:egfp)^{y1}* haploid embryos allowing for straightforward identification of mutant vascular phenotypes (Fig. 1C–G). In total, we screened approximately 1200 mutagenized genomes and identified 17 females that produced clutches in which half of the haploid embryos displayed specific defects in vascular morphology. In all cases, general morphology of the mutant embryos was comparable to their wild type siblings (data not shown). We were able to identify 4 classes of mutant phenotypes in clutches of haploid embryos from F1 *Tg(fli1:egfp)^{y1}* females. Class I mutants such as *y10*, displayed a complete loss of segmental artery formation (Figure 1D, Table 1) while the level of transgene expression was comparable to wild type siblings indicating the presence of endothelial cells within the presumptive dorsal aorta and posterior cardinal vein. In Class II mutants, such as *y16*, we observed partial segmental

artery formation (Figure 1E). A single Class III mutant, *um7*, displayed ectopic branching of segmental arteries (Figure 1F). The *y11* mutant (Class IV) exhibited the most severe effect on vascular development with a complete loss of segmental arteries, defective formation of the major trunk vessels (Figure 1G), as well as loss of cranial blood vessels (data not shown).

To confirm that the vascular defects observed in haploids would persist in diploid embryos and to facilitate genetic mapping, we out-crossed putative F1 female mutant carriers to a genetically diverse wild type line (TL; Figure 1A). We were able to obtain viable F2 families from 14 out of 17 females. In clutches of embryos from 10 out of the 14 families, we observed defective vascular phenotypes that were similar or identical to those observed in mutant haploid embryos (see below). Subsequent bulk segregant analysis, fine genetic mapping and/or candidate cloning revealed 10 distinct alleles in 4 genes that were responsible for the observed vascular defects. The *y11* mutation lies in the endothelial cell specific transcription factor, ets-related protein (*etsrp*), leading to global defects in endothelial gene expression, apoptosis of endothelial cells, and defects in vascular morphogenesis (Pham et al., 2007). Consistent with the ectopic sprouting defects observed in *um7* mutants, we find that this mutation maps to the *plexind1* locus (data not shown), a gene previously implicated in proper segmental artery patterning in zebrafish (Torres-Vazquez et al., 2004). We found that Class I and II mutants that displayed defects in segmental artery formation mapped to two genes implicated in Vegf signaling, *plcg1* and *kdrl*. Based on our previous findings concerning the role of Vegf in artery development, we focused on the detailed genetic and phenotypic characterization of these mutants.

Mutations in a zebrafish Vegf receptor-2 ortholog cause defects in artery development

We have previously found that a mutation in a zebrafish Vegf receptor, referred to as *kdr-like* (previously referred to as *flk1* or *kdra*) is responsible for partial segmental artery defects associated with the *y17* mutant identified in our haploid screen (Table 1(Covassin et al., 2006)). Of the other segmental artery mutants identified in our screen, only *um6* failed to complement *y17* (data not shown), indicating that it also was a mutation in *kdrl*. Interestingly, the *um6* mutation appeared to lead to more severe defects in segmental artery formation in haploid embryos than those associated with *y17* (Table 1). Therefore, to better evaluate the effects of the $kdrl^{um6}$ and $kdrl^{y17}$ mutations on vascular development, we compared them to a null *kdrl* allele that we generated through targeted mutagenesis using zinc finger nucleases (Meng et al., 2008). The *um19* allele is a 4 base pair deletion in exon 2 of *kdrl* and introduces a frameshift that truncates the Kdrl receptor tyrosine kinase in the extracellular domain.

We first compared defects in vascular morphogenesis associated with each *kdrl* allele in mutant embryos bearing the $Tg(fli1:egfp)^{y1}$ transgene. In wild type siblings at 30 hours post fertilization, a basic vascular network consisting of the dorsal aorta, segmental arteries and the dorsal longitudinal anastomotic vessel (DLAV) was evident (Figure 2A). The $kdrl^{um6}$ mutation appeared to have the most severe effect on segmental artery formation leading to variable formation of partial segmental arteries in most embryos (Figure 2B, white arrows indicate partial segmental arteries). In many cases, small filopodial extensions were observed at the usual site of segmental artery formation, but sprouts failed to emanate from the dorsal aorta (Figure 2B, red arrowheads). $kdrl^{um6}$ mutant embryos also failed to display a distinctly separated dorsal aorta and posterior cardinal vein and instead a single major trunk vessel was evident (Figure 2B, red bracket). We observed that defective segmental artery formation due to the null $kdrl^{um19}$ mutation was similar to $kdrl^{um6}$ mutant embryos, although partial sprouts were consistently observed within every segment (Figure 2C). Interestingly, morphogenesis of the dorsal aorta and posterior cardinal vein was largely normal in $kdrl^{um19}$ mutant embryos (Figure 2C). Embryos mutant for $kdrl^{y17}$ displayed the mildest segmental artery defects, with variable formation of DLAVs and partial segmental artery formation evident (Figure 2D).

However, dorsal aorta morphogenesis appeared abnormal as we observed its discontinuous formation in *kdrl*^{y17} mutant embryos (Figure 2D, red arrowhead). This observation is consistent with our previous finding of arteriovenous shunting between the dorsal aorta and posterior cardinal vein in *kdrl*^{y17} mutant embryos (Covassin et al., 2006). Quantification of segmental artery length in each mutant confirmed that the *um6* mutation most severely affected segmental artery formation, while *um19* and *y17* had increasingly milder effects (Figure 2E). Subsequent molecular analysis of the *kdrl* coding sequence in *um6* mutant embryos revealed a T to G transversion resulting in a missense mutation that changed cysteine to glycine at amino acid 1117 within the Kdrl cytoplasmic domain (Table 1). This cysteine residue is identical in the related zebrafish vegf-receptor 2 ortholog, *kdr*, as well as related Vegf receptors in zebrafish, mouse, and human (Figure 2F).

Our analysis of vascular morphology in *kdrl* mutants revealed a surprisingly differential effect on angiogenic formation of segmental arteries and dorsal aorta morphogenesis. To further assess how these alleles affect vascular morphogenesis and function, we assayed circulatory defects in *kdrl* mutant embryos. At 55 hpf, wild type embryos displayed a functional circulatory system that carries hemoglobinized red blood cells (Figure 3A and data not shown). By contrast, *kdrl*^{um6} mutant embryos failed to exhibit any active circulation and display pericardial edema (Figure 3B and data not shown). Closer inspection of embryos derived from *kdrl*^{um6} heterozygous carriers revealed that approximately five percent of all embryos with otherwise normal circulatory flow displayed cranial hemorrhage (compare Figures 3C and D; Figure 3H). Subsequent genotyping of these embryos revealed that they were heterozygous for the T to G transversion (data not shown) suggesting that the *kdrl*^{um6} mutation can act as a mild dominant negative. Despite the moderate severity of the segmental artery defects in *kdrl*^{um19} mutant embryos, this mutation had the mildest effect on circulatory function consistent with normal dorsal aorta morphogenesis in these embryos (Figure 2C). At 55 hpf all *kdrl*^{um19} mutant embryos displayed normal circulation throughout the vascular system with no evidence of cardiac edema (Figure 3E, H). However, cranial hemorrhage was evident in approximately fifteen percent of all embryos, indicating a partially penetrant defect in vascular function in *kdrl*^{um19} mutants (Figure 3G, H). Consistent with our previous study, we observed variable circulatory defects in *kdrl*^{y17} mutant embryos, including some embryos with complete lack of circulation, presence of arteriovenous shunts between the dorsal aorta and posterior cardinal vein, and cranial hemorrhage (Figure 3H and data not shown). Taken together, our results indicate that these alleles differentially affect blood vessel formation in the developing embryo.

Mutations in *phospholipase c gamma 1* perturb artery development

Our previous work demonstrated that the *y10* mutation (Figure 1C, Table 1) lies in a splice donor site within the *phospholipase c gamma 1* (*plcg1*) gene leading to a specific defect in artery development (Lawson et al., 2003). Plcg1 mediates signaling downstream of a number of different receptor tyrosine kinases, including receptors for platelet derived growth factors (Pdgfs), fibroblast growth factors (Fgfs) and Vegf itself (Rhee, 2001; Wilde and Watson, 2001). Plcg1 interacts with phosphorylated tyrosine residues on an activated receptor tyrosine kinase via its SH2 domains. Subsequent activation of Plcg1 occurs through phosphorylation of tyrosine residues by the upstream receptor tyrosine kinase. This results in induction of Plcg1 catalytic activity leading to cleavage of phosphoinositide-4,5-bisphosphate (PIP2) to form inositol-3-phosphate (IP3) and diacylglycerol (DAG), second messengers that ultimately induce calcium release and activation of protein kinase C isoforms, respectively (Rhee, 2001). More recently, Plcg1 has been shown to transduce signals mediated by other upstream activators through interaction with its SH3 domain and can function in a catalytic domain independent manner in this regard (Patterson et al., 2002; Ye et al., 2002).

We found that five additional mutants failed to complement *plcg1*^{y10} or displayed genetic linkage to *plcg1* (data not shown and Table 1). The *y13*, *y15*, and *y16* alleles are point mutations in the *plcg1* coding sequence that change conserved amino acid residues in relevant functional domains (Table 1; Fig. 4A and data not shown). Both *plcg1*^{y13} and *plcg1*^{y15} are in the X region of the split catalytic domain essential for lipase activity (Rhee, 2001). In *y13* mutant embryos C_{412} is mutated to R, while *y15* changes I_{383} to N. In both cases, these residues are identical in the catalytic domains of related phospholipases across a wide variety of species (Figure 4A and data not shown). The *plcg1*^{y16} mutation changes R_{557} to H in the N terminal Src homology 2 (SH2) domain. Based on crystal structure of the homologous SH2 domain in Src (Waksman et al., 1993), this residue is important for direct binding to phosphorylated tyrosine residues. The *y18* allele is a G to A transition in the consensus splice donor site (GT) for exon ENSDARE00000761392 (ENSEMBL, Zv7) and leads to a deletion in the X catalytic domain and premature truncation of the coding sequence (Figure 4A and data not shown). The *y19* mutation results in a small deletion in the *plcg1* coding sequence, although we have not identified the genomic lesion in this mutant.

All *plcg1* mutant embryos exhibited specific defects in artery development, but overall normal morphology was normal (data not shown). Wild type sibling embryos displayed a fully formed segmental artery network at 30 hpf (Figure 4B) while embryos mutant for *plcg1*^{y13} (Figure 4C) or *plcg1*^{y18} (Figure 4E) failed to form segmental artery sprouts. In addition, *plcg1*^{y13} and *plcg1*^{y18} mutant embryos do not initiate blood circulation. Consistent with the observed haploid phenotype (see Figure 1E), the *plcg1*^{y16} mutation caused weaker defects in artery development as all mutant embryos display partial segmental artery sprouts at 30 hpf (Fig. 4D). Most embryos mutant for *plcg1*^{y16} failed to initiate circulation, although we observed mutant embryos with arteriovenous shunts between the dorsal aorta and posterior cardinal vein (data not shown).

Plcg1 can mediate Vegf signaling through direct interaction with Kdr in human endothelial cells (Takahashi et al., 2001) and can also interact with the related Vegf receptor, Flt4 (Borg et al., 1995). Accordingly, we have found that combined loss of Kdrl and Flt4 recapitulates segmental artery phenotype observed in *plcg1* mutant zebrafish embryos(Covassin et al., 2006). However, these observations do not rule out the possibility that Plcg1 mediates signaling through other signaling molecules through interaction with its SH3 domain. Therefore, to investigate this possibility, we performed an *in vivo* rescue assay using forms of *plcg1* containing point mutations within the N-SH2 (R581K), C-SH2 (R689K) or SH3 (P837L) domains. Similar mutations in identical residues in mammalian *plcg1* abrogate the function of these domains and prevent downstream signaling (Ji et al., 1999; Patterson et al., 2002; Ye et al., 2002). We injected mRNA encoding mutant forms of *plcg1* into embryos derived from an incross of *plcg1*^{y18} heterozygous embryos (Figure 4F). We then assayed for segmental artery formation at 30 hpf and circulation at 55 hpf, followed by PCR-based genotyping. All uninjected *plcg1*^{y18} mutant embryos failed to exhibit segmental artery formation or circulation, while injection of mRNA encoding wild type Plcg1 rescued these defects in the majority of mutant embryos (Figure 4G, H). Injection of mRNA encoding Plcg1 containing either SH2 mutations failed to rescue segmental artery formation or circulation (Figure 4G, H). By contrast, mutant embryos injected with *plcg1* mRNA containing the P837L mutation in the SH3 domain were rescued to a similar degree as wild type *plcg1*. These results demonstrate that the SH3 domain is dispensable for Plcg1 signaling during vascular development. Taken together with the characterization of *plcg1* mutants, our observations are consistent with a necessary role for Plcg1 catalytic activity downstream of receptor tyrosine kinases such as Kdrl and Flt4 during vascular development.

Signaling molecules that can be activated as a result of Vegf signaling through Plcg1 include Akt and components the MAP kinase cascade (Zachary and Gliki, 2001). Additionally, recent

observations in zebrafish suggest that MAPK signaling is important for artery development (Hong et al., 2006). Therefore, we investigated whether activation of either of these pathways could rescue vascular defects downstream of *plcg1*. To activate the MAPK cascade, we expressed a version of mitogen activated protein kinase kinase 1 (MAP2K1) containing amino acid substitutions (Ser218>Glu and Ser222>Asp; referred to hereafter as actMAP2K1; Supplemental Figure 1) that lead to 20-fold increases in activity of its downstream substrate, MAPK1 (Mansour et al., 1994). Accordingly, embryos injected with mRNA encoding a mCherrry fluorescent protein-actMAP2K1 fusion display overt defects in development as a consequence of ubiquitous MAPK activation (Supplemental Figure 2C–H). To avoid these early developmental effects, we drove expression of mCherry-actMAP2K1 in endothelial cells using the *fli1ep* cis element in a Tol2-transposon backbone (Villefranc et al., 2007). Wild type embryos expressing *mCherry-actMAP2K1* displayed red fluorescence throughout the trunk vasculature (Figure 5A–C), including the segmental arteries. In some cases, segmental arteries expressing high levels of the transgene appeared to exhibit increased filopodial activity, while those expressing lower levels were normal (Figure 5A, B). In *plcg1*^{y13} mutant embryos, cells expressing *fli1ep:mCherry-actMAP2K1* could be found within blood vessels (Figure 5D–F). However, *mCher-actMAP2K1*-positive cells did not form segmental arteries, despite their ability to contribute to the dorsal roof of the aorta in *plcg1*^{y13} mutant embryos (see arrows in Figure 5E, F). Similarly, we did not observe circulation in *plcg1*^{y13} mutant embryos expressing *fli1ep*-driven *mCher-actMAP2K1*, even in cases of low transgene mosaicism (data not shown).

To determine if Akt could rescue vascular defects downstream of *plcg1,* we expressed a myristoylated form of this kinase that leads to its constitutive activation (referred to as mAkt, (Kohn et al., 1996)). To monitor expression of mAkt, we generated a cassette containing the viral 2A sequence in between mAkt and monomeric Cherry fluorescent protein (*mAkt-2A-mCher*; Supplemental Figure 1), allowing expression of these two separate proteins from a single transcript (Provost et al., 2007). As with activated MAP2K1, injection of mRNA encoding *mAkt-2A-mCher* led to overt defects on embryonic development (Supplemental Figure 2I–L). Therefore, we again used the *fli1ep* element to drive expression of *mAkt-2A-mCher* in endothelial cells. As with actMAPK21, we were able to observe mAkt-2A-mCher-expressing cells in the wild type vasculature of *Tg(fli1a:egfp)*^{y1} embryos (data not shown). Similarly, endothelial cells expressing *mAkt-2A-mCher* could localize to the aorta, but failed to initiate segmental artery sprout formation in *plcg1*^{y13} mutant embryos (Figure 5G–I) or rescue circulation (data not shown). Taken together, these results indicate that activation of either MAPK or Akt signaling alone does not appear to be sufficient downstream of *plcg1* to rescue vascular development.

We have previously reported that *plcg1*^{y10} mutant embryos display only partially penetrant defects in arterial endothelial differentiation, while defects in circulation and segmental artery formation are observed in all mutant embryos (Lawson et al., 2003). To determine if the other alleles of *plcg1* lead to similar arterial endothelial differentiation defects, we assayed artery marker gene expression in embryos at 24 hpf, followed by genotypic analysis to identify mutant and wild type siblings. We observed that differences in artery marker gene expression could be separated into three phenotypic classes in embryos derived from *plcg1* mutant heterozygous incrosses: normal (Figure 6A), weak (Figure 6B), or absent (Figure 6C). Following genotyping, we found that all wild type sibling embryos displayed normal artery specific expression of both *ephrinb2a* and *notch3* (Figure 6D). By contrast more than half of *plcg1*^{y13} and *plcg1*^{y18} mutant embryos displayed complete loss of or weak artery marker gene expression, although the remaining mutant embryos expressed normal levels (Figure 6D). Consistent with the weaker artery defects in *plcg1*^{y16} mutants, we observed a higher proportion of *ephrinb2a* and *notch3* expression in these embryos (Fig. 6D).

The partially penetrant defects in artery differentiation suggested to us that maternally deposited *plcg1* transcript (Tsang et al., 2004) could partially compensate for zygotic loss of *plcg1* in our mutants. To investigate this possibility, we performed germline replacement (Ciruna et al., 2002) to generate adult zebrafish that would produce *plcg1* homozygous null gametes. We then crossed maternal mutant (M*plcg1*^{y18}) and paternal mutant (P*plcg1*^{y18}) carriers and observed progeny embryos for defects in overall morphology, vascular function, and artery marker gene expression. Embryos derived from M*plcg1*^{y18} x P*plcg1*^{y18} crosses (referred to as MPZ*plcg1*^{y18}) displayed relatively normal morphology at 30 hpf (Fig. 6E). While collapsed brain ventricles (arrows in Figure 6E, F) were evident in MPZ*plcg1*^{y18} mutant embryos, other morphological landmarks within the brain, such as the mid-brain hindbrain boundary were evident, suggesting that Fgf signaling was normal (Reifers et al., 2000). Incomplete filling of the ventricles has been observed in mutants lacking circulation(Lowery and Sive, 2005) and can be seen in *kdrl*^{um6} mutant embryos (see Figure 3B). Within the trunk of MPZ*plcg1*^{y18} embryos, development of the neural tube, floor plate, and notochord, as well as pigmentation, appeared normal (Fig. 6G). However, all embryos derived from M*plcg1*^{y18} x P*plcg1*^{y18} crosses failed to initiate circulation, displayed a disorganized dorsal aorta and posterior cardinal vein and exhibited cardiac edema at 55 hpf (data not shown). By contrast, embryos derived from a cross between a M*plcg1*^{y18} female and a wild type *Tg(fli1a:egfp)*^{y1} male yielded all normal embryos that did not exhibit any vascular defects (Figure 6F, H, data not shown). To determine if maternal *plcg1* could rescue arterial specification in the absence of zygotic gene function, we assayed artery maker gene expression (*ephrinb2a* and *dll4*) in MPZ*plcg1*^{y18} embryos. Interestingly, we observed consistent variation in the penetrance of artery differentiation defects between two different M*plcg1*^{y18} female carriers. However, in both cases loss of artery marker gene expression was more severe in MPZ*plcg1*^{y18} embryos than in zygotic *plcg1*^{y18} (Figure 6D). Embryos derived from one of the M*plcg1*^{y18} female carrier failed to express either *ephrinb2a* or *dll4*, while nearly half of the embryos from the second M*plcg1*^{y18} female carrier displayed weak artery marker gene expression (Figure 6D). We did not observe normal artery marker gene expression in any MPZ*plcg1*^{y18} embryos. These results suggest that maternal *plcg1* contribution alone is largely dispensable for embryonic development. However, in the absence of zygotic *plcg1*, maternal contribution appears capable of providing a compensatory signal that can rescue artery differentiation.

Plcg1 can mediate Vegf receptor signaling in endothelial cell lines (Takahashi et al., 2001) and our previous work suggests that *plcg1* is required for Vegf responsiveness in zebrafish embryos (Lawson et al., 2003). However, an endothelial cell autonomous function for *plcg1* has not been demonstrated. Therefore, we performed mosaic analysis using cell transplantation in zebrafish embryos to investigate the requirement for *plcg1* in endothelial cells. For this purpose, we utilized two endothelial cell specific transgenic lines. As a source of donor cells, we relied on *Tg(fli1a:egfp)*^{y1} transgenic embryos. For host embryos, we used *Tg(fli1ep:dsredex)*^{um13} transgenic embryos in which the *fli1ep* element (Villefranc et al., 2007) drives expression of the red fluorescent protein, dsRedExpress, in all endothelial cells. As a general cell lineage tracer, we injected all donor embryos at the 1-cell stage with Cascade Blue. At sphere stage, cells were removed from *Tg(fli1a:egfp)*^{y1} donor embryos and transplanted into similarly staged *Tg(fli1ep:dsredex)*^{um13} recipients (Supplemental Figure 3). We then assayed for contribution of Egfp-positive donor cells in the red vasculature of host embryos between 25 to 28 hpf. We find that wild type *Tg(fli1a:egfp)*^{y1} donor cells are capable of contributing to all blood vessel types within the trunk vasculature when transplanted into wild type *Tg(fli1ep:dsredex)*^{um13} recipients (Figure 7A, Table 2). To determine if *plcg1* was required autonomously in endothelial cells, we generated Plcg1-deficient host by injection of a *plcg1* Morpholino followed by transplantation as described (Supplemental Figure 3). We observed that wild type *Tg(fli1a:egfp)*^{y1} cells could contribute to segmental arteries in embryos otherwise lacking *plcg1*, while host red fluorescent segmental arteries were not observed (Figure 7B). This result indicates that Plcg1 functions autonomously within endothelial cells to mediate segmental

artery sprouting. To determine if *plcg1* deficient cells could contribute to wild type blood vessels, we performed the converse transplantation experiment. In this case, we co-injected Plcg1 MO and Cascade Blue to generate *plcg1*-deficient *Tg(fli1a:egfp)*^{y1} donor embryos (Supplemental Figure 3). In the resulting embryos, we failed to observe any *plcg1* deficient Egfp-positive cells in segmental arteries (Table 2). However, *plcg1*-deficient cells were capable of contributing to other trunk blood vessels, including the dorsal aorta and posterior cardinal vein (Figure 7C, Table 2). Interestingly, we found that *plcg1* deficient cells in dorsal aorta were more likely to contribute to the ventral wall than to the dorsal wall of this blood vessel (Figure 7D). Similarly, we observed that transplanted cells mutant for *plcg1*^{y13} could localize the ventral wall of the aorta (Figure 7E, Table 2).

Discussion

In this work we describe a forward genetic approach to identify vascular mutants using the zebrafish as a model system. Our screening strategy combined two particular aspects of the zebrafish model that proved beneficial: first, the use of a transgenic line expressing Egfp in endothelial cells allowing robust and direct visualization of blood vessel morphology in live embryos (Lawson and Weinstein, 2002). Second, the ability to rapidly screen mutagenized genomes by generating haploid embryos from F1 females. Despite the haploid genotype in the embryos we were scoring, we found that this approach can reliably identify mutations affecting vascular development. We were able to identify several specific classes of vascular defects in haploid *Tg(fli1a:egfp)*^{y1} embryos, including loss of segmental artery formation as well as ectopic branching of these vessels. It was also possible to identify milder defects in segmental artery sprouting and these were consistent with phenotypes associated with hypomorphic mutations in *kdrl* and *plcg1* in diploid embryos. We observed that the majority of putative haploid mutant phenotypes were recapitulated in diploid embryos. Furthermore, we eliminated many other vascular phenotypes during screening based on obvious morphological defects in other tissues. Consistently, the mutant phenotypes we observed in diploid *Tg(fli1a:egfp)*^{y1} embryos were specific to the vascular system. Thus, it is possible to utilize a transgenic haploid screening strategy in zebrafish to reliably identify mutations that affect tissue-specific morphogenetic processes. The increasing availability of cell type-specific transgenic lines should allow this approach to be applied toward the genetic analysis of morphogenesis or differentiation in other organs and tissues in the developing zebrafish embryo.

Several groups have previously utilized the zebrafish to identify mutations affecting cardiovascular function and morphogenesis. In initial large-scale mutagenesis screens, two groups working in parallel identified zebrafish mutants lacking normal circulation using simple visual inspection by light microscopy (Chen et al., 1996; Stainier et al., 1996). By using a two-generation screening approach in which circulatory phenotypes were scored in the progeny of F2 families (a so-called “F3 screen”), these groups identified approximately 70 loci that affected cardiovascular function from nearly 6000 mutagenized genomes. More recently, Jin et al. have incorporated transgenic visualization of endothelial cells into an F3 screening strategy (Jin et al., 2007). In this case, circulatory defects were first screened in F3 progeny of non-transgenic fish, followed by visualization of the vascular system via alkaline phosphatase staining. Identified F2 carriers were then crossed into the *Tg(kdrl:egfp)*^{s843} background (Jin et al., 2005) to visualize the vasculature in more detail. This approach led to the identification of 30 loci that affected blood vessel formation out of approximately 4000 genomes screened. In each screen, the number of identified loci also included mutants that affected other tissues, in addition to blood vessels. Given that our screen focused on blood vessel specific defects, the number of loci per mutagenized genome that we identified using the haploid transgenic approach are similar.

The central drawback to F3 screening approaches in zebrafish is that they are cost- and labor-intensive, require significant amounts of tank space, and generally take up to 5 years to screen sufficient numbers of mutant genomes. The transgenic haploid screening approach we describe here can be performed by a small lab group within a much shorter time frame. Furthermore, confirmation of diploid phenotypes can be performed in a map-cross background, making preliminary genetic mapping much more rapid than standard F3 screens. An obvious drawback of the haploid approach is the limitation on possible phenotypes that could be observed in a haploid embryo. In addition, haploid embryos display overt developmental abnormalities and some mutant phenotypes may be adversely affected by gene dosage. That being said, the majority of phenotypes we observed in haploid embryos were evident in diploids and we were able to identify several different phenotypic classes indicating that our screening approach was robust and reliable.

Plcg1 has been implicated in a variety of signaling cascades in a number of different cell types (Rhee, 2001; Wilde and Watson, 2001). In most cases, Plcg1 functions downstream of receptor tyrosine kinases through a canonical pathway that entails binding of the Plcg1 SH2 domains to phosphorylated tyrosine residues within activated receptors, phosphorylation of tyrosine residues on Plcg1 by the upstream kinase, and subsequent induction of Plcg1 catalytic activity (Rhee, 2001). More recently, several studies have revealed new signaling roles for Plcg1 independent of its lipase activity (Patterson et al., 2002; Ye et al., 2002). However, the relevant mode of Plcg1 signaling *in vivo* and during embryonic development is not clear. Previously, we had found that *plcg1* deficient zebrafish embryos displayed specific defects in artery development and failed to respond to exogenous Vegf (Lawson et al., 2003). Similar vascular defects have been observed in *plcg1* null mouse embryos (Liao et al., 2002) further suggesting a primary role for *plcg1* during Vegf signaling and/or vascular development. The specificity of these developmental defects had been surprising based on the extensive range of signaling processes in which *plcg1* was known to play a role. While maternal compensation could explain the specificity of these embryonic defects, we find that this is not the case. Zebrafish embryos lacking maternal *plcg1* develop normally and those that lack zygotic, maternal, and paternal, *plcg1* proceed through gastrulation and are morphologically indistinguishable from zygotic mutants. We did not observe phenotypes associated with deficiency in other receptor tyrosine kinase signaling pathways that act early in development, such as Fgf (Reifers et al., 1998; Tsang et al., 2004) in any of these cases. These observations suggest that the primary role of *plcg1* during animal development is to mediate development of the vascular system. Furthermore, our allelic series and structure/function analysis indicate a canonical mode of Plcg1 signaling downstream of Vegf receptors. Mutations within conserved residues of the Plcg1 catalytic domain result in similar defects associated with the putative null *y18* allele, suggesting that catalytic activity is indispensable for Plcg1 function during vascular development. Furthermore, mutation of the N-SH2 domain leads to similar defects while Plcg1 bearing mutations in either of the SH2 domains fails to rescue the *plcg1* mutant phenotype. Consistent with its presumed role downstream of the Vegf receptors, we demonstrate that *plcg1* function is required autonomously within endothelial cells for proper segmental artery development and artery differentiation. Taken together with our previous observations that *plcg1* mutant embryos fail to respond to exogenous Vegf (Lawson et al., 2003), these results indicate that the primary role for *plcg1* during development is to transduce Vegf signaling during blood vessel formation.

Several lines of evidence indicate that the Vegf signaling pathway is providing distinct signals to endothelial cells through Plcg1 at different points during vascular development. We have previously shown that *kdrl* and *plcg1* are essential for artery differentiation or specification (Lawson et al., 2003; Lawson et al., 2002), a process that is known to occur during mid-somitogenesis stages prior to formation of the dorsal aorta (Zhong et al., 2001). Our findings that maternal *plcg1* provides a compensatory signal for differentiation but not morphogenesis,

which occurs during later stages, further supports the action of a Kdrl/Plcg1 signaling pathway during this earlier time point. During later segmental artery morphogenesis both *kdrl* and the zebrafish Vegf receptor-3 ortholog, *flt4*, appear to act through *plcg1* (Covassin et al., 2006; Lawson et al., 2003) as combined loss of these receptors recapitulates the segmental artery and circulatory defects observed in *plcg1* mutant embryos. Whether the different combination of activating receptors (Kdrl versus Kdrl with Flt4) during differentiation and morphogenesis elicit quantitative or qualitative differences in signaling through Plcg1 is not known at this time. The compensatory role of maternal Plcg1 at earlier time points may be most simply explained by a lower threshold of activation required for differentiation versus morphogenesis. In this case, Vegf signaling through Kdrl would lead to lower Plcg1 activity than that associated with both Kdrl and Flt4 during segmental artery sprouting (Figure 8A); in this case higher Plcg1 activity can promote active sprouting, and presumably concomitant differentiation, while lower levels promote differentiation only. Alternatively, the formation of different signaling complexes between the receptors and Plcg1 in these two settings may lead to the activation of distinct downstream signaling molecules and corresponding cellular output (Figure 8B). This possibility would be consistent with the additional role of Plcg1 as an adaptor protein to mediate downstream signaling molecules (Wilde and Watson, 2001). In either case, it is likely that distinct downstream effector molecules are subsequently acting to drive artery differentiation or morphogenesis downstream of Plcg1.

Our characterization of *kdrl* alleles would support the existence of qualitatively distinct signaling outputs in these different developmental contexts. The $kdrl^{um6}$ mutation leads to the most severe defects in both segmental artery formation and circulatory function, as well as cranial hemorrhage in some heterozygous carriers, suggesting that this mutation acts as a mild dominant negative. The severity of the morphogenesis defects in these mutants as compared to the null $kdrl^{um19}$ allele suggests that the *um6* mutant receptor may block signaling of multiple Vegf receptors, including *flt4*, which can heterodimerize with Vegfr-2 in human endothelial cell lines (Alam et al., 2004). The milder effect of the $kdrl^{y17}$ mutation, which eliminates kinase activity (Covassin et al., 2006), is somewhat surprising in this regard since similar mutations in related receptors yield dominant negative forms of these molecules (Dumont et al., 1994; Reith et al., 1993; Reith et al., 1990). Segmental artery formation is more robust in $kdrl^{y17}$ mutants when compared to the null phenotype raising the intriguing possibility that the Kdrl receptor can function in a kinase independent manner during segmental artery sprouting. Despite the loss of kinase activity, the $Kdrl^{y17}$ receptor could still function as an adaptor or substrate for other kinases, such as Flt4, allowing sufficient, albeit compromised, activation of *plcg1* and relatively normal segmental artery formation. In this case, the dominant negative *um6* mutation would be predicted to block the interaction between Kdrl and Flt4, or prevent interaction with downstream effectors. This model would also be consistent with the effects of *y17* on dorsal aorta morphogenesis, which appear more severe than those associated with $kdrl^{um19}$. While *flt4* and *kdrl* are co-expressed in segmental artery tip cells, there is only transient co-expression of both transcripts in the dorsal aorta, followed by potent down-regulation of *flt4* expression. Formation of the dorsal aorta may proceed through the independent function of these receptors and therefore requires kinase activity of the Kdrl receptor. Taken together, our results suggest that Vegf/Plcg1 signaling is acting in distinct signaling contexts during artery differentiation, dorsal aorta morphogenesis and segmental artery sprouting. Further identification of additional alleles in *kdrl*, as well as mutations in *flt4*, will undoubtedly be helpful to dissect the diverse genetic interactions of these receptors and to identify downstream effectors that mediate each of these processes.

The zebrafish has proven to be an ideal model to study vascular development. The ability to perform forward genetic screens for vascular mutants has led to the identification of novel genes and new insights on how blood vessels form during embryonic development. Our demonstration that haploid transgenic screening allows reliable identification of vascular

mutants will facilitate future screening for new genes affecting this blood vessel formation. By incorporating new transgenic lines that are more lineage-restricted within the vasculature, it would be possible to further expand the range of phenotypic classes that could be identified. For example, use of artery or vein restricted transgenes may yield additional classes of mutations that affect endothelial differentiation without overt defects in vascular morphogenesis; these mutants would not have been easily identified in our screen. While the forward genetic approach has proven valuable, it is likely that new reverse genetic approaches will begin to be more widely applied. The size of the zebrafish genome precludes saturation screening and numerous mutants have now been repeatedly isolated from several different screens. The number of genes expressed in cardiovascular tissue in zebrafish embryos numbers well over 100, with many more likely to be identified. Moving forward, a concerted effort that integrates focused transgene-assisted forward genetic screens, along with reverse approaches that take advantage of new technologies (e.g. zinc finger nucleases for genome modification) will allow for a comprehensive genetic analysis of endothelial cell development and vascular morphogenesis.

Supplementary Material

Refer to Web version on PubMed Central for supplementary material.

Acknowledgments

We would like to thank the members of the NIH and UMass Screen Teams: NIH – Brianne Lo, Josh Mugford, Michael Tsang, Neil Hukriede and Sue Lyons; UMass – Letitiah Etheridge, Seong-Kyu Choe, Kristen Alexa, Nicolas Hirsch and Charles Sagerstrom. We thank John Polli for outstanding fish care. We thank Fumihiko Urano, Roger Davis, Alex Schier, Erez Raz, and Chi-Bin Chien for generously providing plasmids used in this study. This work was supported by R01CA107454 (National Cancer Institute) awarded to N. D. L. and a Ruth Kirchstein Minority Predoctoral Fellowship (F31HL081927; National Heart, Lung, and Blood Institute) awarded to J.A.V.

References

Adams RH, Wilkinson GA, Weiss C, Diella F, Gale NW, Deutsch U, Risau W, Klein R. Roles of ephrinB ligands and EphB receptors in cardiovascular development: demarcation of arterial/venous domains, vascular morphogenesis, and sprouting angiogenesis. Genes Dev 1999;13:295–306. [PubMed: 9990854]

Alam A, Herault JP, Barron P, Favier B, Fons P, Delesque-Touchard N, Senegas I, Laboudie P, Bonnin J, Cassan C, Savi P, Ruggeri B, Carmeliet P, Bono F, Herbert JM. Heterodimerization with vascular endothelial growth factor receptor-2 (VEGFR-2) is necessary for VEGFR-3 activity. Biochem Biophys Res Commun 2004;324:909–15. [PubMed: 15474514]

Alt B, Elsalini OA, Schrumpf P, Haufs N, Lawson ND, Schwabe GC, Mundlos S, Gruters A, Krude H, Rohr KB. Arteries define the position of the thyroid gland during its developmental relocalisation. Development 2006;133:3797–804. [PubMed: 16968815]

Bates DO, Harper SJ. Regulation of vascular permeability by vascular endothelial growth factors. Vascul Pharmacol 2002;39:225–37. [PubMed: 12747962]

Beis D, Stainier DY. In vivo cell biology: following the zebrafish trend. Trends Cell Biol 2006;16:105–12. [PubMed: 16406520]

Borg JP, deLapeyriere O, Noguchi T, Rottapel R, Dubreuil P, Birnbaum D. Biochemical characterization of two isoforms of FLT4, a VEGF receptor- related tyrosine kinase. Oncogene 1995;10:973–84. [PubMed: 7898938]

Bussmann J, Lawson N, Zon L, Schulte-Merker S. Zebrafish VEGF receptors: a guideline to nomenclature. PLoS Genet 2008;4:e1000064. [PubMed: 18516225]

Carmeliet P, Ferreira V, Breier G, Pollefeyt S, Kieckens L, Gertsenstein M, Fahrig M, Vandenhoeck A, Harpal K, Eberhardt C, Declercq C, Pawling J, Moons L, Collen D, Risau W, Nagy A. Abnormal blood vessel development and lethality in embryos lacking a single VEGF allele. Nature 1996;380:435–9. [PubMed: 8602241]

Carmeliet P, Ng YS, Nuyens D, Theilmeier G, Brusselmans K, Cornelissen I, Ehler E, Kakkar VV, Stalmans I, Mattot V, Perriard JC, Dewerchin M, Flameng W, Nagy A, Lupu F, Moons L, Collen D, D'Amore PA, Shima DT. Impaired myocardial angiogenesis and ischemic cardiomyopathy in mice lacking the vascular endothelial growth factor isoforms VEGF164 and VEGF188. Nat Med 1999;5:495–502. [PubMed: 10229225]

Chen JN, Haffter P, Odenthal J, Vogelsang E, Brand M, van Eeden FJ, Furutani-Seiki M, Granato M, Hammerschmidt M, Heisenberg CP, Jiang YJ, Kane DA, Kelsh RN, Mullins MC, Nusslein-Volhard C. Mutations affecting the cardiovascular system and other internal organs in zebrafish. Development 1996;123:293–302. [PubMed: 9007249]

Ciruna B, Weidinger G, Knaut H, Thisse B, Thisse C, Raz E, Schier AF. Production of maternal-zygotic mutant zebrafish by germ-line replacement. Proc Natl Acad Sci U S A 2002;99:14919–24. [PubMed: 12397179]

Cleaver, O.; Krieg, PA. Molecular mechanisms of vascular development. In: Harvey, RP.; Rosenthal, N., editors. Heart Development. Academic Press; San Diego: 1999. p. 221-252.

Covassin LD, Villefranc JA, Kacergis MC, Weinstein BM, Lawson ND. Distinct genetic interactions between multiple Vegf receptors are required for development of different blood vessel types in zebrafish. Proc Natl Acad Sci U S A 2006;103:6554–9. [PubMed: 16617120]

Davis S, Aldrich TH, Jones PF, Acheson A, Compton DL, Jain V, Ryan TE, Bruno J, Radziejewski C, Maisonpierre PC, Yancopoulos GD. Isolation of angiopoietin-1, a ligand for the TIE2 receptor, by secretion-trap expression cloning. Cell 1996;87:1161–9. [PubMed: 8980223]

Dumont DJ, Gradwohl G, Fong GH, Puri MC, Gertsenstein M, Auerbach A, Breitman ML. Dominant-negative and targeted null mutations in the endothelial receptor tyrosine kinase, tek, reveal a critical role in vasculogenesis of the embryo. Genes Dev 1994;8:1897–909. [PubMed: 7958865]

Ferrara N, Gerber HP, LeCouter J. The biology of VEGF and its receptors. Nat Med 2003;9:669–76. [PubMed: 12778165]

Gerety SS, Wang HU, Chen ZF, Anderson DJ. Symmetrical mutant phenotypes of the receptor EphB4 and its specific transmembrane ligand ephrin-B2 in cardiovascular development. Mol Cell 1999;4:403–14. [PubMed: 10518221]

Hauptmann G, Gerster T. Two-color whole-mount in situ hybridization to vertebrate and Drosophila embryos. Trends Genet 1994;10:266. [PubMed: 7940754]

Hong CC, Peterson QP, Hong JY, Peterson RT. Artery/vein specification is governed by opposing phosphatidylinositol-3 kinase and MAP kinase/ERK signaling. Curr Biol 2006;16:1366–72. [PubMed: 16824925]

Imai Y, Feldman B, Schier AF, Talbot WS. Analysis of chromosomal rearrangements induced by postmeiotic mutagenesis with ethylnitrosourea in zebrafish. Genetics 2000;155:261–72. [PubMed: 10790400]

Ji QS, Chattopadhyay A, Vecchi M, Carpenter G. Physiological requirement for both SH2 domains for phospholipase C-gamma1 function and interaction with platelet-derived growth factor receptors. Mol Cell Biol 1999;19:4961–70. [PubMed: 10373546]

Jin SW, Beis D, Mitchell T, Chen JN, Stainier DY. Cellular and molecular analyses of vascular tube and lumen formation in zebrafish. Development 2005;132:5199–209. [PubMed: 16251212]

Jin SW, Herzog W, Santoro MM, Mitchell TS, Frantsve J, Jungblut B, Beis D, Scott IC, D'Amico LA, Ober EA, Verkade H, Field HA, Chi NC, Wehman AM, Baier H, Stainier DY. A transgene-assisted genetic screen identifies essential regulators of vascular development in vertebrate embryos. Dev Biol 2007;307:29–42. [PubMed: 17531218]

Kawakami K, Takeda H, Kawakami N, Kobayashi M, Matsuda N, Mishina M. A transposon-mediated gene trap approach identifies developmentally regulated genes in zebrafish. Dev Cell 2004;7:133–44. [PubMed: 15239961]

Kohn AD, Takeuchi F, Roth RA. Akt, a pleckstrin homology domain containing kinase, is activated primarily by phosphorylation. J Biol Chem 1996;271:21920–6. [PubMed: 8702995]

Kwan KM, Fujimoto E, Grabher C, Mangum BD, Hardy ME, Campbell DS, Parant JM, Yost HJ, Kanki JP, Chien CB. The Tol2kit: a multisite gateway-based construction kit for Tol2 transposon transgenesis constructs. Dev Dyn 2007;236:3088–99. [PubMed: 17937395]

Lammert E, Cleaver O, Melton D. Induction of pancreatic differentiation by signals from blood vessels. Science 2001;294:564–7. [PubMed: 11577200]

Lawson ND, Mugford JW, Diamond BA, Weinstein BM. phospholipase C gamma-1 is required downstream of vascular endothelial growth factor during arterial development. Genes Dev 2003;17:1346–51. [PubMed: 12782653]

Lawson ND, Scheer N, Pham VN, Kim CH, Chitnis AB, Campos-Ortega JA, Weinstein BM. Notch signaling is required for arterial-venous differentiation during embryonic vascular development. Development 2001;128:3675–83. [PubMed: 11585794]

Lawson ND, Vogel AM, Weinstein BM. sonic hedgehog and vascular endothelial growth factor act upstream of the Notch pathway during arterial endothelial differentiation. Dev Cell 2002;3:127–36. [PubMed: 12110173]

Lawson ND, Weinstein BM. In vivo imaging of embryonic vascular development using transgenic zebrafish. Dev Biol 2002;248:307–318. [PubMed: 12167406]

Lee S, Chen TT, Barber CL, Jordan MC, Murdock J, Desai S, Ferrara N, Nagy A, Roos KP, Iruela-Arispe ML. Autocrine VEGF signaling is required for vascular homeostasis. Cell 2007;130:691–703. [PubMed: 17719546]

Liao HJ, Kume T, McKay C, Xu MJ, Ihle JN, Carpenter G. Absence of erythrogenesis and vasculogenesis in Plcg1-deficient mice. J Biol Chem 2002;277:9335–41. [PubMed: 11744703]

Lowery LA, Sive H. Initial formation of zebrafish brain ventricles occurs independently of circulation and requires the nagie oko and snakehead/atp1a1a.1 gene products. Development 2005;132:2057–67. [PubMed: 15788456]

Maisonpierre PC, Suri C, Jones PF, Bartunkova S, Wiegand SJ, Radziejewski C, Compton D, McClain J, Aldrich TH, Papadopoulos N, Daly TJ, Davis S, Sato TN, Yancopoulos GD. Angiopoietin-2, a natural antagonist for Tie2 that disrupts in vivo angiogenesis. Science 1997;277:55–60. [PubMed: 9204896]

Mansour SJ, Matten WT, Hermann AS, Candia JM, Rong S, Fukasawa K, Vande Woude GF, Ahn NG. Transformation of mammalian cells by constitutively active MAP kinase kinase. Science 1994;265:966–70. [PubMed: 8052857]

Meng X, Noyes MB, Zhu LJ, Lawson ND, Wolfe SA. Targeted gene inactivation in zebrafish using engineered zinc-finger nucleases. Nat Biotechnol 2008;26:695–701. [PubMed: 18500337]

Patterson RL, van Rossum DB, Ford DL, Hurt KJ, Bae SS, Suh PG, Kurosaki T, Snyder SH, Gill DL. Phospholipase C-gamma is required for agonist-induced Ca2+ entry. Cell 2002;111:529–41. [PubMed: 12437926]

Patton EE, Zon LI. The art and design of genetic screens: zebrafish. Nat Rev Genet 2001;2:956–66. [PubMed: 11733748]

Pham VN, Lawson ND, Mugford JW, Dye L, Castranova D, Lo B, Weinstein BM. Combinatorial function of ETS transcription factors in the developing vasculature. Dev Biol 2007;303:772–83. [PubMed: 17125762]

Provost E, Rhee J, Leach SD. Viral 2A peptides allow expression of multiple proteins from a single ORF in transgenic zebrafish embryos. Genesis 2007;45:625–9. [PubMed: 17941043]

Quinn TP, Peters KG, De Vries C, Ferrara N, Williams LT. Fetal liver kinase 1 is a receptor for vascular endothelial growth factor and is selectively expressed in vascular endothelium. Proc Natl Acad Sci U S A 1993;90:7533–7. [PubMed: 8356051]

Reifers F, Bohli H, Walsh EC, Crossley PH, Stainier DY, Brand M. Fgf8 is mutated in zebrafish acerebellar (ace) mutants and is required for maintenance of midbrain-hindbrain boundary development and somitogenesis. Development 1998;125:2381–95. [PubMed: 9609821]

Reifers F, Walsh EC, Leger S, Stainier DY, Brand M. Induction and differentiation of the zebrafish heart requires fibroblast growth factor 8 (fgf8/acerebellar). Development 2000;127:225–35. [PubMed: 10603341]

Reith AD, Ellis C, Maroc N, Pawson T, Bernstein A, Dubreuil P. 'W' mutant forms of the Fms receptor tyrosine kinase act in a dominant manner to suppress CSF-1 dependent cellular transformation. Oncogene 1993;8:45–53. [PubMed: 8380922]

Reith AD, Rottapel R, Giddens E, Brady C, Forrester L, Bernstein A. W mutant mice with mild or severe developmental defects contain distinct point mutations in the kinase domain of the c-kit receptor. Genes Dev 1990;4:390–400. [PubMed: 1692559]

Rhee SG. Regulation of phosphoinositide-specific phospholipase C. Annu Rev Biochem 2001;70:281–312. [PubMed: 11395409]

Roman BL, Pham VN, Lawson ND, Kulik M, Childs S, Lekven AC, Garrity DM, Moon RT, Fishman MC, Lechleider RJ, Weinstein BM. Disruption of acvrl1 increases endothelial cell number in zebrafish cranial vessels. Development 2002;129:3009–19. [PubMed: 12050147]

Roman BL, Weinstein BM. Building the vertebrate vasculature: research is going swimmingly. Bioessays 2000;22:882–93. [PubMed: 10984714]

Semenza GL. Angiogenesis in ischemic and neoplastic disorders. Annu Rev Med 2003;54:17–28. [PubMed: 12359828]

Shalaby F, Rossant J, Yamaguchi TP, Gertsenstein M, Wu XF, Breitman ML, Schuh AC. Failure of blood-island formation and vasculogenesis in Flk-1-deficient mice. Nature 1995;376:62–6. [PubMed: 7596435]

Siekmann AF, Covassin L, Lawson ND. Modulation of VEGF signalling output by the Notch pathway. Bioessays 2008;30:303–13. [PubMed: 18348190]

Siekmann AF, Lawson ND. Notch signalling limits angiogenic cell behaviour in developing zebrafish arteries. Nature 2007;445:781–4. [PubMed: 17259972]

Solnica-Krezel L, Schier AF, Driever W. Efficient recovery of ENU-induced mutations from the zebrafish germline. Genetics 1994;136:1401–20. [PubMed: 8013916]

Stainier DY, Fouquet B, Chen JN, Warren KS, Weinstein BM, Meiler SE, Mohideen MA, Neuhauss SC, Solnica-Krezel L, Schier AF, Zwartkruis F, Stemple DL, Malicki J, Driever W, Fishman MC. Mutations affecting the formation and function of the cardiovascular system in the zebrafish embryo. Development 1996;123:285–92. [PubMed: 9007248]

Stalmans I, Ng YS, Rohan R, Fruttiger M, Bouche A, Yuce A, Fujisawa H, Hermans B, Shani M, Jansen S, Hicklin D, Anderson DJ, Gardiner T, Hammes HP, Moons L, Dewerchin M, Collen D, Carmeliet P, D'Amore PA. Arteriolar and venular patterning in retinas of mice selectively expressing VEGF isoforms. J Clin Invest 2002;109:327–36. [PubMed: 11827992]

Suri C, Jones PF, Patan S, Bartunkova S, Maisonpierre PC, Davis S, Sato TN, Yancopoulos GD. Requisite role of angiopoietin-1, a ligand for the TIE2 receptor, during embryonic angiogenesis. Cell 1996;87:1171–80. [PubMed: 8980224]

Suri C, McClain J, Thurston G, McDonald DM, Zhou H, Oldmixon EH, Sato TN, Yancopoulos GD. Increased vascularization in mice overexpressing angiopoietin-1. Science 1998;282:468–71. [PubMed: 9774272]

Takahashi T, Yamaguchi S, Chida K, Shibuya M. A single autophosphorylation site on KDR/Flk-1 is essential for VEGF-A- dependent activation of PLC-gamma and DNA synthesis in vascular endothelial cells. Embo J 2001;20:2768–78. [PubMed: 11387210]

Torres-Vazquez J, Gitler AD, Fraser SD, Berk JD, Van NP, Fishman MC, Childs S, Epstein JA, Weinstein BM. Semaphorin-plexin signaling guides patterning of the developing vasculature. Dev Cell 2004;7:117–23. [PubMed: 15239959]

Tsang M, Maegawa S, Kiang A, Habas R, Weinberg E, Dawid IB. A role for MKP3 in axial patterning of the zebrafish embryo. Development 2004;131:2769–79. [PubMed: 15142973]

Villefranc JA, Amigo J, Lawson ND. Gateway compatible vectors for analysis of gene function in the zebrafish. Dev Dyn 2007;236:3077–87. [PubMed: 17948311]

Waksman G, Shoelson SE, Pant N, Cowburn D, Kuriyan J. Binding of a high affinity phosphotyrosyl peptide to the Src SH2 domain: crystal structures of the complexed and peptide-free forms. Cell 1993;72:779–90. [PubMed: 7680960]

Wang HU, Chen ZF, Anderson DJ. Molecular distinction and angiogenic interaction between embryonic arteries and veins revealed by ephrin-B2 and its receptor Eph-B4. Cell 1998;93:741–53. [PubMed: 9630219]

Weinstein BM, Lawson ND. Arteries, veins, Notch, and VEGF. Cold Spring Harb Symp Quant Biol 2002;67:155–62. [PubMed: 12858536]

Westerfield, M. The Zebrafish Book. University of Oregon Press; Eugene, Oregon: 1993.

Wilde JI, Watson SP. Regulation of phospholipase C gamma isoforms in haematopoietic cells: why one, not the other? Cell Signal 2001;13:691–701. [PubMed: 11602179]

Yancopoulos GD, Davis S, Gale NW, Rudge JS, Wiegand SJ, Holash J. Vascular-specific growth factors and blood vessel formation. Nature 2000;407:242–8. [PubMed: 11001067]

Yancopoulos GD, Klagsbrun M, Folkman J. Vasculogenesis, angiogenesis, and growth factors: ephrins enter the fray at the border. Cell 1998;93:661–4. [PubMed: 9630209]

Ye K, Aghdasi B, Luo HR, Moriarity JL, Wu FY, Hong JJ, Hurt KJ, Bae SS, Suh PG, Snyder SH. Phospholipase C gamma 1 is a physiological guanine nucleotide exchange factor for the nuclear GTPase PIKE. Nature 2002;415:541–4. [PubMed: 11823862]

Zachary I, Gliki G. Signaling transduction mechanisms mediating biological actions of the vascular endothelial growth factor family. Cardiovasc Res 2001;49:568–81. [PubMed: 11166270]

Zhong TP, Childs S, Leu JP, Fishman MC. Gridlock signalling pathway fashions the first embryonic artery. Nature 2001;414:216–20. [PubMed: 11700560]

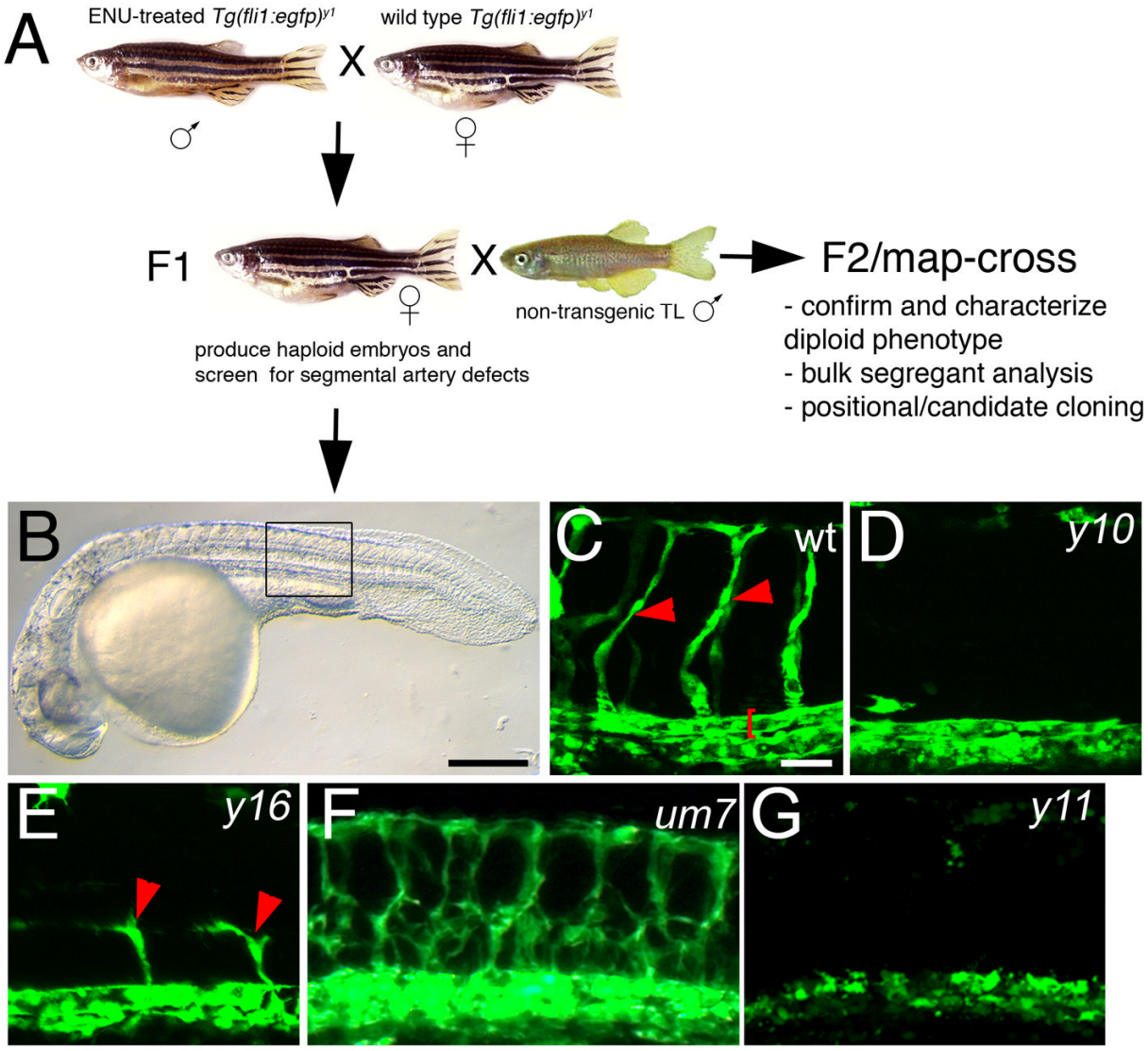

Figure 1.

A transgenic haploid screen for vascular mutants. A. Breeding strategy for transgenic haploid screen. B. Transmitted light image of a *Tg(fli1a:egfp)*^{y1} haploid embryo. C. Segmental arteries (red arrowheads) in a wild type *Tg(fli1a:egfp)*^{y1} haploid embryo. Red bracket denotes dorsal aorta. D. Loss of segmental arteries in a *y10* mutant haploid embryo. E. Partial segmental artery sprouts (red arrowheads) in a *y16* mutant haploid embryo. F. Excessive segmental artery branching in a *um7* mutant haploid embryo. G. Loss of segmental artery formation and failure to form the dorsal aorta in a *y11* haploid mutant embryo. B–G. Lateral views, anterior to the left, dorsal is up. C, D, E G. Confocal fluorescent micrographs. F. Epifluorescent image. B. Scale bar is 250 μM. C–G. Scale bar is 50 μM.

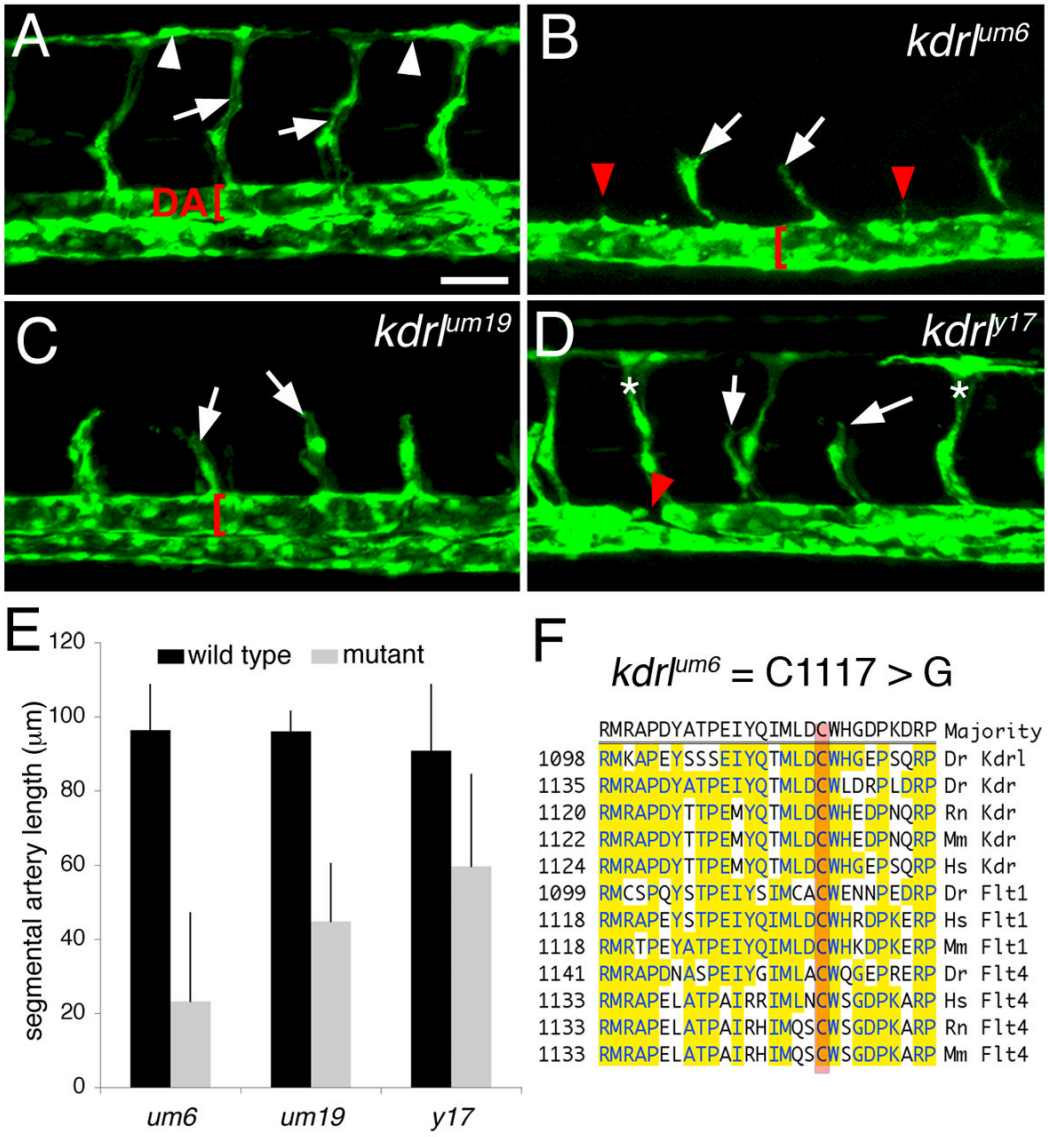

Figure 2.

Mutations in *kdrl* affect segmental artery formation. A.-D. Confocal fluorescent micrographs of zebrafish embryonic trunk blood vessels at 30 hours post fertilization. Lateral views, anterior to the left, dorsal is up. Scale bar is 50 μM A. Wild type *Tg(fli1a:egfp)*^{y1} diploid sibling embryo. Arrowheads indicate DLAV. Arrows denote segmental arteries and dorsal aorta (DA) is indicated by a red bracket. B. Segmental arteries in a *kdrl*^{um6};*Tg(fli1a:egfp)*^{y1} diploid mutant embryo. Partial segmental arteries indicated by white arrows. Red arrowheads indicate somite boundaries at which segmental arteries failed to sprout. Red bracket indicates a trunk vessel with a single lumen. C. Partial segmental artery formation (white arrows) in a *kdrl*^{um19};*Tg (fli1a:egfp)*^{y1} diploid mutant embryo. A well-formed dorsal aorta (red bracket) is apparent in this embryo. D. A *kdrl*^{y17};*Tg(fli1a:egfp)*^{y1} diploid mutant embryo with both fully formed (indicated by asterisks) and partial segmental arteries (white arrows). The red arrow indicates region of the dorsal aorta that is discontinuous. E. Quantification of sprout length in *kdrl* mutant embryos and their wild type siblings. F. Location of the *um6* mutation within the zebrafish Kdrl cytoplasmic domain. ClustalW alignment of conserved regions from Vegf-receptor-2/ Kdr and Vegf-receptor-3/Flt4 from zebrafish (Dr), human (Hs), rat (Rn), and mouse.

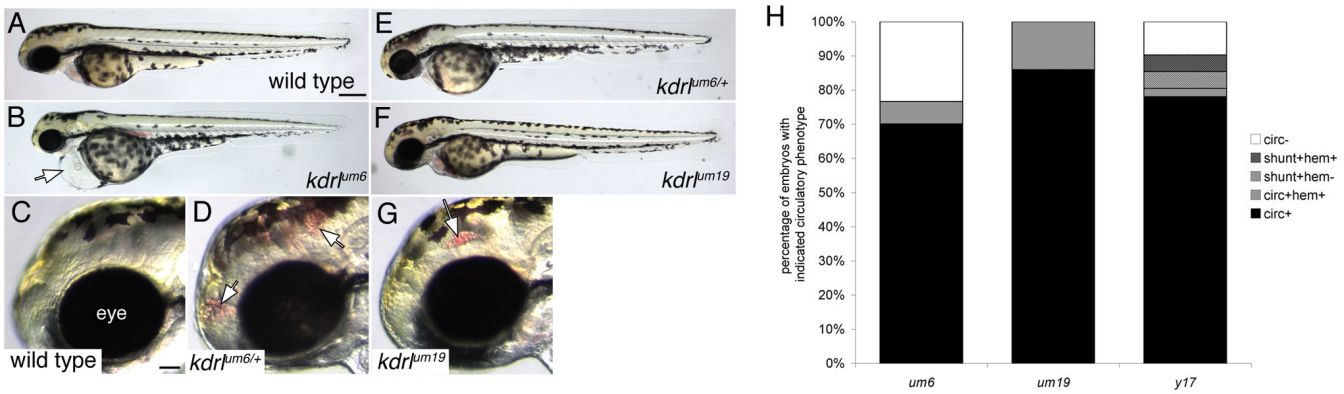

Figure 3.

Defects in circulatory function in *kdrl* mutants. A–G. Transmitted light images of wild type and *kdrl* mutant zebrafish embryos at 55 hours post fertilization. Lateral views, anterior to the left, dorsal is up. A. Wild type sibling embryo. Scale bar is 250 μM. B. *kdrl*^{um6} mutant embryo displaying cardiac edema (white arrow). C. Eye (indicated) and forebrain region of wild type sibling embryo. Scale bar is 50 μM. D. Cranial hemorrhage (white arrows) in a heterozygous carrier of the *kdrl*^{um6} allele. E. *kdrl*^{um6} heterozygous embryo. F. *kdrl*^{um19} mutant embryo. G. Eye and forebrain region of a *kdrl*^{um19} mutant embryo. A cranial hemorrhage is indicated by the white arrow. H. Quantification of circulatory defects in clutches of embryos derived from in-crosses of *um6*, *um19*, and *y17* heterozygous carriers; circ - circulation, shunt - abnormal circulatory connection between dorsal aorta and posterior cardinal vein, hem - cranial hemorrhage.

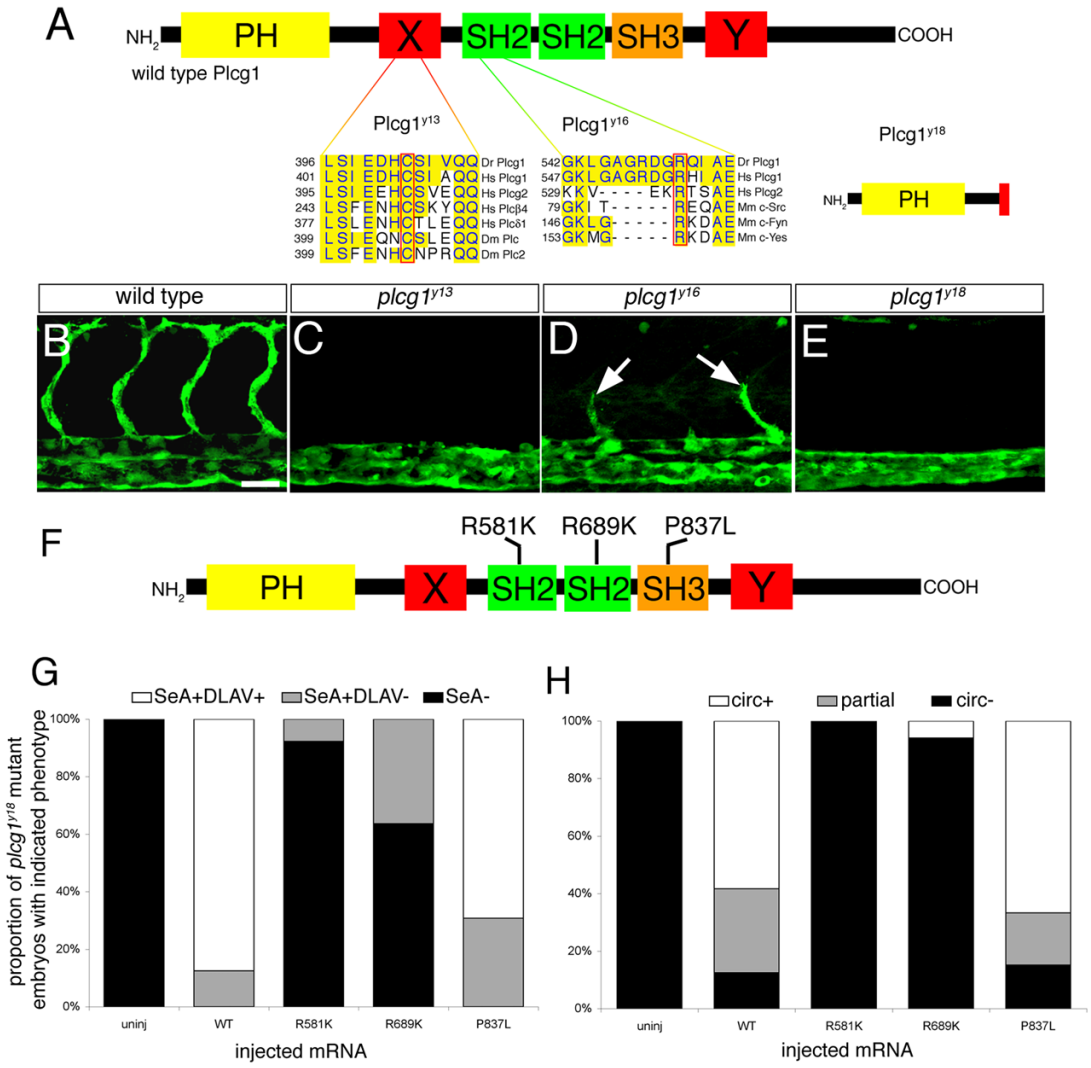

Figure 4.

plcg1 is required for segmental artery formation. A. Functional domains within Plcg1. PH – pleckstrin homology domain; X, Y – split catalytic domains; SH2 – src homology-2 domains; SH3 – src homology 3 domain. Residues affected by the *y13* and *y16* mutations are outlined in red and aligned with conserved sequences from other species (Dr – zebrafish, Hs – human, Dm – Drosophila, Mm – mouse). The *y18* allele leads to a truncation in the X-catalytic domain. B–E. Confocal fluorescent micrographs of trunk blood vessels at 30 hours post fertilization. Lateral views, anterior to the left, dorsal is up. B. Wild type sibling embryo. Scale bar is 50 μM. C. Loss of segmental arteries in a *plcg1*^{y13} mutant embryo. D. Partial segmental arteries (white arrows) in a *plcg1*^{y16} mutant embryo. E. *plcg1*^{y18} mutant embryo. F. Position of point mutations engineered into rescue constructs in the Plcg1 SH2 and SH3 domains. G. Graph indicating proportion of embryos displaying segmental artery or DLAV formation following injection with mRNA encoding the indicated Plcg1 construct. H. Graph indicating proportion of embryos displaying partial or complete circulation following injection with mRNA encoding the indicated Plcg1 construct; SeA - segmental arteries, DLAV - dorsal longitudinal anastamotic vessel, circ - circulation, partial - shunt between dorsal aorta and posterior cardinal vein.

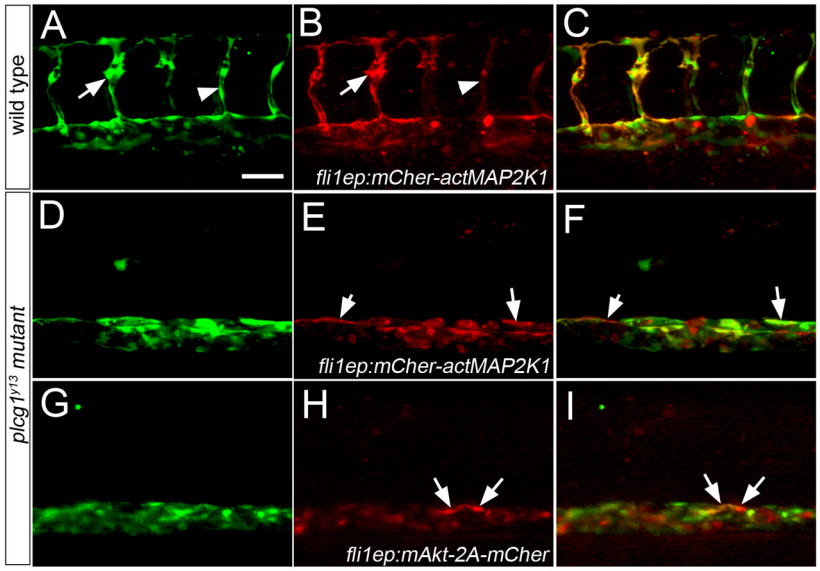

Figure 5.

Activation of Akt or MAPK signaling fails to rescue segmental artery formation in *plcg1*^{y13} mutant embryos. A–I. Confocal fluorescent micrographs of trunk blood vessels at 30 hours post fertilization. Anterior is to the left, dorsal is up. Scale bar is 60 μM. A–C. Wild type *Tg (fli1a:egfp)*^{y1} embryo co-injected with 25 pg Tol2 transposase mRNA and pTol-*fli1ep:mCher-actMAP2K1*; arrow denotes excessive filopodial extensions in a sprout expressing high levels of the transgene; arrowhead is a low transgene expressing cell. D–F. *Tg (fli1a:egfp)*^{y1}*;plcg1*^{y13} mutant embryo co-injected with 25 pg Tol2 transposase mRNA and pTol-*fli1ep:mCher-actMAP2K1*. E, F. Arrows indicate transgene-expressing cells in the dorsal wall of the aorta. G–I. *Tg(fli1a:egfp)*^{y1}*;plcg1*^{y13} mutant embryo co-injected with 25 pg Tol2 transposase mRNA and pTol-*fli1ep:mAkt-2A-mCher*; H, I. Arrows denote transgene expressing cells in the dorsal aorta.

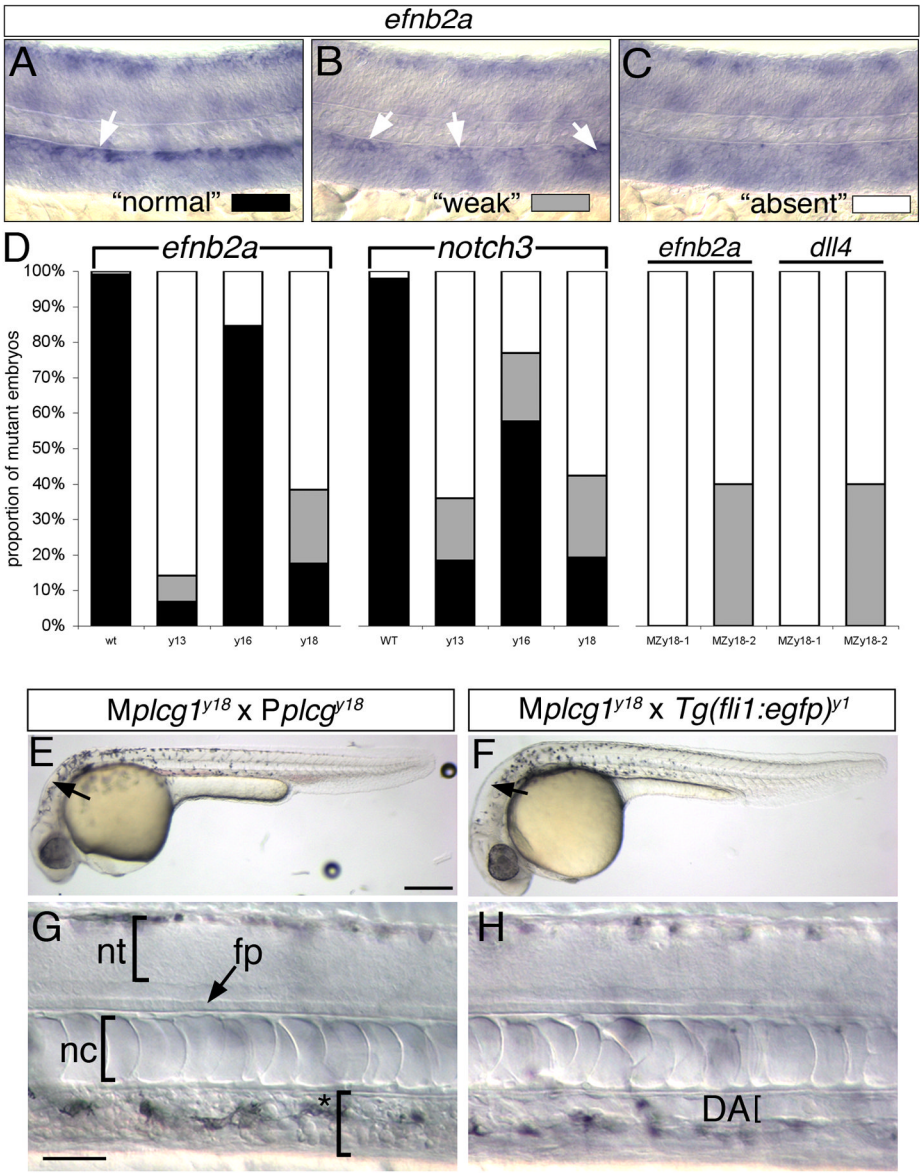

Figure 6.

Artery differentiation defects in *plcg1* mutants. A–C. Classification schema to categorize level of artery marker gene expression in *plcg1* mutant embryos. Differential interference contrast (DIC) images of zebrafish embryo trunks following whole mount in situ hybridization to detect *ephrinb2a* (*efnb2a*). A. Normal *ephrinb2a* expression in the dorsal aorta (white arrow). B. Weak ephrinb2a in distinct patches within the dorsal aorta (white arrows). C. Loss of dorsal *ephrinb2a* expression classified as "absent". D. Quantification of artery marker gene expression in *y13*, *y16*, *y18* and MPZ*y18* mutant embryos. E, F. Transmitted light images of embryos at 30 hpf. Scale bar is 250 μM. G, H. DIC images of embryos at 30 hpf. E–H., Lateral views, anterior to the left, dorsal is up. E, G. *MPZplcg1*^{y18} mutant embryo. Scale bar is 30 μM; nt – neural tube, fp – floor plate, nc – notochord. Asterisked bracket denoted absence of defined dorsal aorta or posterior cardinal vein. F, H. *Mplcg1*^{y18}*; Tg(fli1a:egfp)*^{y1} mutant embryo; DA – dorsal aorta, indicated by a bracket.

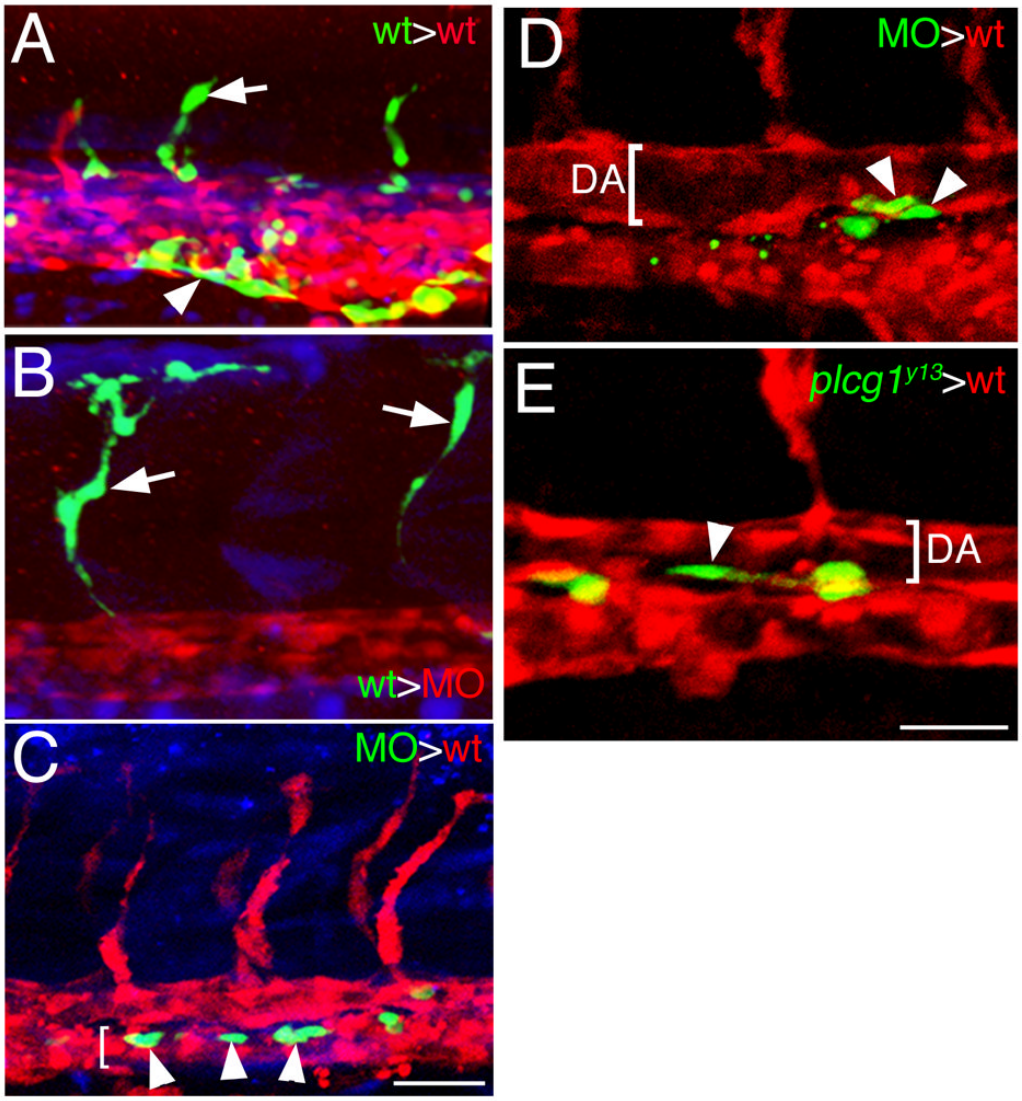

Figure 7.

Plcg1 is required autonomously in endothelial cells for segmental artery sprouting. A.-E. Confocal fluorescent micrographs of trunk blood vessels at approximately 27 hpf. Lateral views, anterior to the left, dorsal is up. In all images, host cells are expressing dsRedEx (red), while donor cells are expressing enhanced green fluorescent protein (green); in A–C, donor cells are also labeled with Cascade Blue (blue). A. Control embryo derived from transplantation of wild type donor *Tg(fli1a:egfp)*^{y1} cells into a *Tg(fli1ep:dsredex)*^{um13} host. Donor contribution to a developing segmental artery (white arrow) and the caudal vein (white arrowhead) is indicated. B. Contribution of donor *Tg(fli1a:egfp)*^{y1} cells to a segmental artery (white arrow) in a *plcg1* MO injected *Tg(fli1ep:dsredex)*^{um13} host. C. Donor *plcg1*-MO injected *Tg (fli1a:egfp)*^{y1} cells (white arrows) within the posterior cardinal vein (lumen indicated by a white bracket) in a wild type *Tg(fli1ep:dsredex)*^{um13} host. D. Donor plcg1-MO injected *Tg (fli1a:egfp)*^{y1} cells (white arrowheads) within the ventral wall of the dorsal aorta (DA, lumen denoted by a white bracket) in a wild type *Tg(fli1ep:dsredex)*^{um13} host. E. Donor *Tg (fli1a:egfp)*^{y1}*;plcg1*^{y13} mutant cells (white arrowheads) within the ventral wall of the dorsal aorta (DA, lumen denoted by a white bracket) in a wild type *Tg(fli1ep:dsredex)*^{um13} host. A–C. Scale bar is 50 μM. D, E. Scale bar is 30 μM.

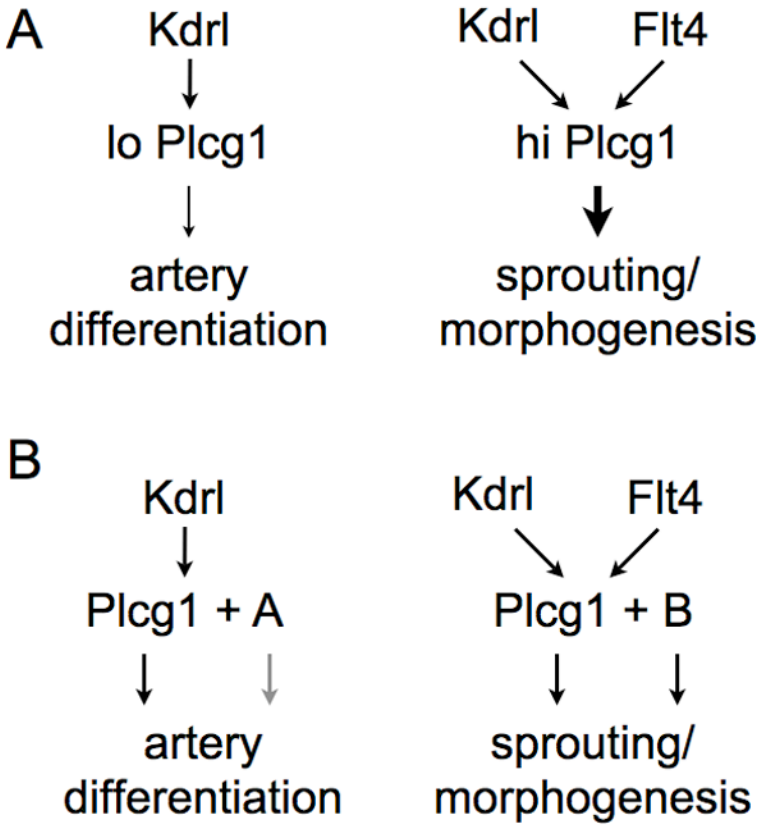

Figure 8.
Model of possible quantitative or qualitative differences of signaling through Plcg1.

Table 1

Segmental artery mutants identified by haploid transgenic screening

Class	gene	allele	mutation	affected domain	SeA	Reference
I	*kdrl*	*um6*	C_{1117}→G	cytoplasmic	none	Meng et al.; this study
	plcg1	*y10*	SA	PH	none	Lawson et al.
		y13	C_{412}→R	X-catalytic	none	this study
		y15	I_{383}→N	X-catalytic	none	-
		y18	SD	all	none	Covassin et al.; this study
		y19	ND	all	none	-
II	*kdrl*	*y17*	L_{846}→R	ATP binding	partial	Covassin et al.; this study
	plcg1	*y16*	R_{557}→H	N-SH2	partial	this study
III	*plexinD1*	*um7*	ND	ND	ectopic	-
IV	*etsrp*	*y11*	insertion	DNA binding	partial	Pham et al.

SA – splice acceptor; SD – splice donor; ND – not determined.

Dev Biol. Author manuscript; available in PMC 2010 May 15.

Table 2

Number of host *Tg(fli1ep:dsredex)*^{um13} embryos displaying donor *Tg(fli1a:egfp)*^{y1} endothelial cells in indicated blood vessel.

		Aorta			
	vein	**ventral**	**dorsal**	**SeA**	**DLAV**
wt>wt	8	8	13	13	5
wt>plcg1 MO	5	7	8	15	5
plcg1 MO>wt	7	11	3	0	0
plcg1^{y13}>wt	2	3	0	0	0

vein – localization in the cardinal or caudal vein; SeA – segmental artery; DLAV – dorsal longitudinal anastamotic vessel. Total numbers: wt into wt, n=15; wt into plcg1 MO, n=27; plcg1 MO into wt, n=19; *plcg1*^{y13} into wt, n=3.